Physica B 404 (2009) 1383–1393

Contents lists available at ScienceDirect

Physica B

journal homepage: www.elsevier.com/locate/physb

# Refraction angles and transmission rates of polarized superluminal radiation

Roman Tomaschitz *

*Department of Physics, Hiroshima University, 1-3-1 Kagami-yama, Higashi-Hiroshima 739-8526, Japan*

ARTICLE INFO

*Article history:*
Received 29 October 2008
Received in revised form
9 December 2008
Accepted 22 December 2008

*PACS:*
42.25.Bs
42.25.Gy
52.25.Mq
95.30.Gv

*Keywords:*
Superluminal wave propagation
Tachyonic Maxwell equations
Boundary conditions for radiation modes with negative mass-square
Transversal and longitudinal refraction
Polarization of tachyonic γ-rays
Tachyonic plasma frequency
Nonthermal cascade spectra

ABSTRACT

The propagation of superluminal waves in dispersive media is investigated, in particular the refraction at surfaces of discontinuity in layered dielectrics. The negative mass-square of the tachyonic modes is manifested in the transmission and reflection coefficients, and the polarization of the incident waves (TE, TM, or longitudinal) can be determined from the refraction angles. The conditions for total internal reflection in terms of polarization and tachyon mass are derived. Brewster angles can be used to discriminate longitudinal from transversal incidence. Superluminal transmission through dielectric boundary layers is studied, and the dependence of the intensity maxima on the transversal and longitudinal refractive indices of the layer is analyzed. Estimates of the tachyonic plasma frequency and permittivity of metals are given. The integral version of the tachyonic Maxwell equations is stated, boundary conditions at the surfaces of discontinuity are derived for transversal and longitudinal wave propagation, and singular surface fields and currents are pointed out. The spectral maps of three TeV γ-ray sources associated with supernova remnants, which have recently been obtained with imaging atmospheric Cherenkov detectors, are fitted with tachyonic cascade spectra. The transversal and longitudinal polarization components are disentangled in the spectral maps, and the thermodynamic parameters of the shock-heated ultra-relativistic electron plasma generating the tachyon flux are extracted from the cascade fits.



## 1. Introduction

We investigate the refraction of superluminal wave modes in dispersive media, at dielectric interfaces and boundary layers. The formalism is developed in analogy to electromagnetic theory [1], even though there are substantial differences due to the negative mass-square of tachyons [2–5] and the occurrence of longitudinally polarized modes [6,7]. The tachyon mass shows in deflection angles, transmission coefficients, and in longitudinal refraction. The superluminal radiation field is a real Proca field with negative mass-square [8]. In 3D, the wave modes can be written in terms of field strengths and inductions, suggesting a counterpart to Maxwell's equations. The tachyonic Maxwell equations explicitly depend on the scalar and vector potentials, so that the gauge invariance is broken. We derive differential and integral field equations, including the material equations in a dispersive medium relating the tachyonic field strengths and potentials to inductions via frequency-dependent permeabilities.

The field equations, the polarization of superluminal modes, and the transversal and longitudinal Poynting vectors of the tachyon flux in a dispersive medium are discussed in Section 2. The transversal and longitudinal refractive indices for tachyonic wave propagation in dielectrics are introduced, and estimates of the tachyonic conductivity of metals are given. Refraction properties such as deflection and reflection angles are determined by boundary conditions on the tachyon potential, the field strengths, and inductions at the surface of discontinuity. There are two types of boundary conditions depending on the polarization of the wave fields, and singular magnetic field strengths and boundary currents can emerge. This is explained in Section 3.

In Section 4, we study superluminal refraction at a plane interface generated by a discontinuity in the permeabilities. The reflection and refraction angles depend on the polarization of the incident modes, and so do the transmission rates. The Brewster angles for transversal and longitudinal incidence are derived, as well as the conditions for total internal reflection of polarized superluminal radiation. The tachyon flux through a dielectric boundary layer is investigated, in particular the intensity peaks at normal incidence. We calculate the transmission and reflection coefficients, and discuss their frequency dependence and the effect of polarization.

In Section 5, we point out evidence for superluminal γ-rays in the spectral maps of three Galactic TeV sources obtained with the imaging air Cherenkov detectors HESS and MAGIC [9–11]. The

* Tel.: +81 824 247361; fax: +81 824 240717.
*E-mail address:* tom@geminga.org

0921-4526/$ - see front matter © 2009 Elsevier B.V. All rights reserved.
doi:10.1016/j.physb.2008.12.026

spectra are fitted with nonthermal tachyonic cascades generated by the shocked electron plasma of the remnants. The transversal and longitudinal polarization components of the cascades are resolved, exhibiting extended spectral plateaus in the high GeV region typical for tachyonic $\gamma$-ray emitters, followed by nonthermal power–law slopes at low TeV energies. The spectral break terminating the GeV plateau is compared to the break energies of the cosmic-ray spectrum. In Section 6, we present our conclusions.

## 2. Tachyonic Maxwell equations and integral field equations in a permeable medium

The tachyonic radiation field in vacuum is a real vector field with negative mass-square, satisfying the Proca equation $(\partial^\nu\partial_\nu + m_t^2)A_\mu = -j_\mu$, subject to the Lorentz condition $A^\mu_{,\mu} = 0$. $m_t$ is the mass of the superluminal Proca field $A_\mu$, and $q$ the tachyonic charge carried by the subluminal electron current $j^\mu = (\rho, \mathbf{j})$. The mass term is added with a positive sign, and the sign convention for the metric defining the d'Alembertian $\partial^\nu\partial_\nu$ is diag $(-1,1,1,1)$, so that $m_t^2 > 0$ is the negative mass-square of the radiation field [6,12]. The above wave equation in conjunction with the Lorentz condition is equivalent to the tachyonic Maxwell equations

$$\operatorname{div}\mathbf{B}(\mathbf{x},t) = 0, \quad \operatorname{rot}\mathbf{E} + \partial\mathbf{B}/\partial t = 0,$$
$$\operatorname{div}\mathbf{E} = \rho - m_t^2 A_0, \quad \operatorname{rot}\mathbf{B} - \partial\mathbf{E}/\partial t = \mathbf{j} + m_t^2\mathbf{A}, \tag{2.1}$$

where the field strengths are related to the potentials by $\mathbf{E} = \nabla A_0 - \partial\mathbf{A}/\partial t$ and $\mathbf{B} = \operatorname{rot}\mathbf{A}$. In contrast to electromagnetic theory, the Lorentz condition $\operatorname{div}\mathbf{A} - \partial A_0/\partial t = 0$ follows from the field equations and current conservation, $\operatorname{div}\mathbf{j} + \partial\rho/\partial t = 0$, cf. after Eq. (2.3).

In a permeable medium, the potentials and field strengths in the inhomogeneous vacuum equations (2.1) are replaced by inductions, $(A_0, \mathbf{A}) \to (C_0, \mathbf{C})$, $(\mathbf{E}, \mathbf{B}) \to (\mathbf{D}, \mathbf{H})$, defined by material equations [13,14]. We will mostly consider monochromatic waves, $\mathbf{A}(\mathbf{x},t) = \hat{\mathbf{A}}(\mathbf{x},\omega)\,\mathrm{e}^{-\mathrm{i}\omega t} + \text{c.c.}$, and analogously for the scalar potential, current, charge density, field strengths, and inductions. Fourier amplitudes are denoted by a hat. Maxwell's equations in Fourier space read

$$\operatorname{rot}\hat{\mathbf{E}} - \mathrm{i}\omega\hat{\mathbf{B}} = 0, \quad \operatorname{div}\hat{\mathbf{B}} = 0,$$
$$\operatorname{rot}\hat{\mathbf{H}} + \mathrm{i}\omega\hat{\mathbf{D}} = \hat{\mathbf{j}} + m_t^2\hat{\mathbf{C}}, \quad \operatorname{div}\hat{\mathbf{D}} = \hat{\rho} - m_t^2\hat{C}_0, \tag{2.2}$$

supplemented by material equations

$$\hat{\mathbf{A}}(\omega) = \mu_0(\omega)\hat{\mathbf{C}}(\omega), \quad \hat{C}_0(\omega) = \varepsilon_0(\omega)\hat{A}_0(\omega),$$
$$\hat{\mathbf{D}}(\mathbf{x},\omega) = \varepsilon(\omega)\hat{\mathbf{E}}(\mathbf{x},\omega), \quad \hat{\mathbf{B}}(\mathbf{x},\omega) = \mu(\omega)\hat{\mathbf{H}}(\mathbf{x},\omega). \tag{2.3}$$

The inductive potentials $(\hat{C}_0, \hat{\mathbf{C}})$ as well as the inductions $\hat{\mathbf{D}}$ and $\hat{\mathbf{H}}$ are related to the primary fields by frequency-dependent dielectric $(\varepsilon_0, \varepsilon)$ and magnetic $(\mu_0, \mu)$ permeabilities. The Fourier amplitudes of the field strengths and potentials are connected by $\hat{\mathbf{E}} = \mathrm{i}\omega\hat{\mathbf{A}} + \nabla\hat{A}_0$ and $\hat{\mathbf{B}} = \operatorname{rot}\hat{\mathbf{A}}$. We take the divergence of the third equation in Eq. (2.2), and substitute the fourth, to obtain

$$\mu_0(\mathrm{i}\omega\hat{\rho} - \operatorname{div}\hat{\mathbf{j}}) = m_t^2(\operatorname{div}\hat{\mathbf{A}} + \mathrm{i}\omega\varepsilon_0\mu_0\hat{A}_0). \tag{2.4}$$

Current conservation, $\operatorname{div}\hat{\mathbf{j}} = \mathrm{i}\omega\hat{\rho}$, implies the Lorentz condition $\operatorname{div}\hat{\mathbf{A}} + \mathrm{i}\varepsilon_0\mu_0\omega\hat{A}_0 = 0$, or equivalently, $\mathrm{i}\omega\hat{C}_0 + \operatorname{div}\hat{\mathbf{C}} = 0$ in terms of the inductive potentials.

The sign conventions for the coupling of an electron to the Proca field are $L = -m/\gamma + q(A_0 + \mathbf{A}\cdot\mathbf{v})$ and $m\mathrm{d}(\gamma\mathbf{v})/\mathrm{d}t = q(\mathbf{E} + \mathbf{v}\times\mathbf{B})$, where $\gamma = (1-\upsilon^2)^{-1/2}$ is the electronic Lorentz factor and $q$ the tachyonic charge carried by the electron, cf. after Eq. (2.14). The primary fields rather than the inductions define the Lorentz force. The potentials are unambiguously determined by the field strengths and the dielectric and magnetic permeabilities. We define polarizations $\hat{\mathbf{P}}$, $\hat{\mathbf{M}}$, and $(\hat{Q}_0, \hat{\mathbf{Q}})$, relating the inductions and field strengths additively as $\hat{\mathbf{D}} = \hat{\mathbf{E}} + \hat{\mathbf{P}}$ and $\hat{\mathbf{B}} = \hat{\mathbf{H}} + \hat{\mathbf{M}}$, and analogously the potentials $\hat{\mathbf{A}} = \hat{\mathbf{C}} + \hat{\mathbf{Q}}$ and $\hat{C}_0 = \hat{A}_0 + \hat{Q}_0$. Accordingly, $\hat{\mathbf{P}} = \kappa\hat{\mathbf{E}}$ and $\hat{Q}_0 = \kappa_0\hat{A}_0$, with electric susceptibilities $\kappa = \varepsilon - 1$ and $\kappa_0 = \varepsilon_0 - 1$. Analogously, $\hat{\mathbf{M}} = \chi\hat{\mathbf{H}}$ and $\hat{\mathbf{Q}} = \chi_0\hat{\mathbf{C}}$, with magnetic susceptibilities $\chi = \mu - 1$ and $\chi_0 = \mu_0 - 1$. The permeabilities $\varepsilon_0$ and $\mu_0$ define the inductive potentials in Eq. (2.3), and are not to be confused with vacuum permeabilities; we use the Heaviside–Lorentz system, so that $\varepsilon = \varepsilon_0 = 1$ and $\mu = \mu_0 = 1$ in vacuum.

Applying the Gauss theorem to the divergence equations in Eq. (2.2), as well as to the Lorentz condition and the potential definition of $\hat{\mathbf{E}}$, cf. after Eq. (2.3), we find the integral field equations

$$\int_S \hat{\mathbf{D}}\cdot\mathrm{d}\mathbf{S} = \int_V (m_t^2\hat{C}_0 - \hat{\rho})\mathrm{d}V, \quad \int_S \hat{\mathbf{B}}\cdot\mathrm{d}\mathbf{S} = 0,$$
$$\int_S \hat{\mathbf{C}}\cdot\mathrm{d}\mathbf{S} = \mathrm{i}\omega\int_V \hat{C}_0\mathrm{d}V, \quad \int_S \hat{A}_0\mathrm{d}\mathbf{S} = \int_V (\mathrm{i}\omega\hat{\mathbf{A}} - \hat{\mathbf{E}})\,\mathrm{d}V. \tag{2.5}$$

Here, $\mathrm{d}\mathbf{S} = \mathbf{n}\mathrm{d}S$ is the surface element of a closed surface $S$, the boundary of a domain $V$ with volume element $dV$, and $\mathbf{n}$ is the surface normal pointing into the interior of the domain of integration $V$. Current conservation gives

$$\int_S \hat{\mathbf{j}}\cdot\mathrm{d}\mathbf{S} = -\mathrm{i}\omega\int_V \hat{\rho}\mathrm{d}V, \quad \int_S \mathbf{x}(\hat{\mathbf{j}}\cdot\mathrm{d}\mathbf{S}) = -\int_V (\hat{\mathbf{j}} + \mathrm{i}\omega\mathbf{x}\hat{\rho})\,\mathrm{d}V. \tag{2.6}$$

Applying the Stokes theorem to the rotor equations in Eq. (2.2) and the potential definition of $\hat{\mathbf{B}}$, we obtain

$$\oint_L \hat{\mathbf{H}}\,\mathrm{d}\mathbf{s} = \int_{S_L} (m_t^2\hat{\mathbf{C}} - \mathrm{i}\omega\hat{\mathbf{D}} + \hat{\mathbf{j}})\,\mathrm{d}\mathbf{S},$$
$$\frac{1}{\mathrm{i}\omega}\oint_L \hat{\mathbf{E}}\,\mathrm{d}\mathbf{s} = \oint_L \hat{\mathbf{A}}\,\mathrm{d}\mathbf{s} = \int_{S_L} \hat{\mathbf{B}}\,\mathrm{d}\mathbf{S}. \tag{2.7}$$

Here, $\mathrm{d}\mathbf{S} = \mathbf{n}\mathrm{d}S$ is the surface element of an oriented open surface $S_L$ bounded by the closed loop $L$, and $\mathrm{d}\mathbf{s} = \mathbf{n}\times\mathbf{n}_L\,\mathrm{d}s$ is the oriented tangent element of the loop. $\mathbf{n}_L$ is the unit vector tangent to the surface and orthogonal to the loop, pointing to the exterior. $\mathbf{n}$ is the unit normal of the surface at the loop, with the same orientation as the surface element $\mathrm{d}\mathbf{S}$.

To find the transversal and longitudinal dispersion relations, we use a plane–wave ansatz in the Maxwell equations (2.2) with vanishing charge and current densities: $\hat{\mathbf{A}}(\mathbf{x},\omega) = \mathbf{A}(\mathbf{k})\mathrm{e}^{\mathrm{i}\mathbf{k}\cdot\mathbf{x}}$, and analogously for the scalar potential and the field strengths. Here, $\mathbf{k} = k(\omega)\mathbf{k}_0$, where $k$ is the wave number to be determined from the field equations, and $\mathbf{k}_0$ is a constant unit vector. $k(\omega)$ as well as $\mathbf{k}_0$ can be complex. The transversality condition is $\hat{\mathbf{A}}\cdot\mathbf{k}_0 = 0$, and the set of transversal modes is $\mathbf{A}(\mathbf{x},t) = \hat{\mathbf{A}}^{\mathrm{T}}(\mathbf{x},\omega)\,\mathrm{e}^{-\mathrm{i}\omega t} + \text{c.c.}$, with amplitude $\hat{\mathbf{A}}^{\mathrm{T}}(\mathbf{x},\omega) = \mathbf{A}^{\mathrm{T}}(\mathbf{k})\,\mathrm{e}^{\mathrm{i}k_{\mathrm{T}}\mathbf{k}_0\cdot\mathbf{x}}$, and similarly for the field strengths and the scalar potential. The dispersion relation determining the transversal wave number is

$$k_{\mathrm{T}}^2 = \varepsilon\mu\omega^2 + m_t^2\mu/\mu_0, \tag{2.8}$$

and the amplitudes of the transversal field strengths follow from $\hat{\mathbf{A}}^{\mathrm{T}}$:

$$\mathbf{k}_0\cdot\hat{\mathbf{A}}^{\mathrm{T}} = 0, \quad \hat{A}_0^{\mathrm{T}} = 0, \quad \hat{\mathbf{E}}^{\mathrm{T}} = \mathrm{i}\omega\hat{\mathbf{A}}^{\mathrm{T}}, \quad \hat{\mathbf{B}}^{\mathrm{T}} = \mathrm{i}k_{\mathrm{T}}\mathbf{k}_0\times\hat{\mathbf{A}}^{\mathrm{T}}. \tag{2.9}$$

If the product $\hat{\mathbf{A}}\cdot\mathbf{k}_0$ does not vanish, the modes must be longitudinal, $\hat{\mathbf{A}}^{\mathrm{L}}(\mathbf{x},\omega) = \mathbf{A}^{\mathrm{L}}(\mathbf{k})\mathrm{e}^{\mathrm{i}k_{\mathrm{L}}\mathbf{k}_0\cdot\mathbf{x}}$, with dispersion relation

$$k_{\mathrm{L}}^2 = \varepsilon_0\mu_0\omega^2 + m_t^2\varepsilon_0/\varepsilon \tag{2.10}$$

so that $k_{\rm T}^2/k_{\rm L}^2=\varepsilon\mu/(\varepsilon_0\mu_0)$. The amplitudes of the longitudinal scalar potential and the field strengths read

$$\hat{\mathbf{A}}^{\rm L}=(\hat{\mathbf{A}}^{\rm L}\cdot\mathbf{k}_0)\mathbf{k}_0,\quad \hat{A}_0^{\rm L}=-\frac{k_{\rm L}}{\varepsilon_0\mu_0\omega}\mathbf{k}_0\cdot\hat{\mathbf{A}}^{\rm L},$$
$$\hat{\mathbf{E}}^{\rm L}=\frac{m_t^2}{{\rm i}\varepsilon\mu_0\omega}\hat{\mathbf{A}}^{\rm L},\quad \hat{\mathbf{B}}^{\rm L}=0. \tag{2.11}$$

The amplitudes $\mathbf{A}^{\rm T,L}(\mathbf{k})$ only need to satisfy the transversality/longitudinality condition, that is, the first equation in Eqs. (2.9) and (2.11), respectively.

The time-averaged tachyonic energy flux carried by homogeneous modes (with real wave vector $\mathbf{k}_0$) in a dispersive and non-absorptive medium is

$$\langle\mathbf{S}^{\rm T}\rangle=\frac{2k_{\rm T}}{\mu}\omega|\hat{\mathbf{A}}^{\rm T}|^2\mathbf{k}_0,\quad \langle\mathbf{S}^{\rm L}\rangle=\frac{2k_{\rm L}}{\mu_0^2\varepsilon_0}\frac{m_t^2}{\omega}|\hat{\mathbf{A}}^{\rm L}|^2\mathbf{k}_0, \tag{2.12}$$

where $|\hat{\mathbf{A}}|^2$ stands for $\hat{\mathbf{A}}\cdot\hat{\mathbf{A}}^*$. As above, the superscripts T and L refer to the transversal and longitudinal flux components. The frequency-dependent permeabilities of a dispersive transparent medium are real in the absence of energy dissipation. The flux vectors (2.12) apply even for negative permeabilities [15–17], provided that we restrict to a frequency range where the squared wave numbers (2.8) and (2.10) are positive. They are obtained by substituting the polarized plane waves (2.9) and (2.11) into the Poynting vector $\mathbf{S}=\mathbf{E}\times\mathbf{H}+m_{\rm t}^2A_0\mathbf{C}$, and by performing a time average [18].

The transversal and longitudinal phase velocities read $\upsilon_{\rm ph}^{\rm T,L}=\omega/k_{\rm T,L}$, and the tachyonic group velocities are $\upsilon_{\rm gr}^{\rm T,L}={\rm d}\omega/{\rm d}k_{\rm T,L}$, so that $\upsilon_{\rm gr}^{\rm T}\upsilon_{\rm ph}^{\rm T}=1/(\varepsilon\mu)$ and $\upsilon_{\rm gr}^{\rm L}\upsilon_{\rm ph}^{\rm L}=1/(\varepsilon_0\mu_0)$. In the case of vacuum permeabilities, $\varepsilon_{(0)}=\mu_{(0)}=1$, the transversal and longitudinal velocities coincide, and we find $\omega=m_t\gamma_t$, where $\gamma_t=(\upsilon_{\rm gr}^2-1)^{-1/2}$ denotes the tachyonic Lorentz factor and $\upsilon_{\rm gr}>1$ is the superluminal group velocity. The refractive index $n_{\rm T,L}=k_{\rm T,L}/\omega$, defined as dimensionless inverse phase velocity, differs for transversal and longitudinal modes:

$$n_{\rm T}=\sqrt{\varepsilon\mu+\frac{\mu}{\mu_0}\frac{m_{\rm t}^2}{\omega^2}},\quad n_{\rm L}=\sqrt{\varepsilon_0\mu_0+\frac{\varepsilon_0}{\varepsilon}\frac{m_{\rm t}^2}{\omega^2}}. \tag{2.13}$$

At high frequencies $\omega\gg m_t$ (with $m_{\rm t}\approx 2.15\,{\rm keV}$ [6,18] and $\hbar=c=1$), we can approximate $n_{\rm T}\sim\sqrt{\varepsilon\mu}$. The longitudinal index, $n_{\rm L}\sim\sqrt{\varepsilon_0\mu_0}$, has no electromagnetic analog. In the low-frequency regime $\omega\ll m_t$, the refractive indices are frequency dependent even if the permeabilities stay constant, $n_{\rm T}\sim\sqrt{\mu/\mu_0}m_t/\omega$ and $n_{\rm L}\sim\sqrt{\varepsilon_0/\varepsilon}m_t/\omega$.

To estimate the dielectric permeability for tachyonic wave propagation, we start with a monochromatic superluminal mode, $\mathbf{E}(\mathbf{x},t)=\hat{\mathbf{E}}(\mathbf{x},\omega){\rm e}^{-{\rm i}\omega t}+{\rm c.c.}$, in a dispersive and possibly dissipative medium. This mode generates the current $\hat{\mathbf{j}}=\sigma(\omega)\hat{\mathbf{E}}$, $\hat{\rho}=-{\rm i}(\sigma/\omega){\rm div}\,\hat{\mathbf{E}}$, where $\sigma(\omega)$ is the tachyonic conductivity of the medium, cf. Eq. (2.14). The charge distribution $\hat{\rho}$ is found by means of current conservation, cf. after Eq. (2.4). We substitute this current into the field equations (2.2) with vacuum permeabilities $\varepsilon_{(0)}=\mu_{(0)}=1$, and absorb current and charge density by introducing the permittivity $\varepsilon_\sigma(\omega)=1+{\rm i}\sigma(\omega)/\omega$. In this way, we can write the inhomogeneous field equations (2.2) as ${\rm rot}\,\hat{\mathbf{B}}+{\rm i}\varepsilon_\sigma\omega\hat{\mathbf{E}}=m_t^2\hat{\mathbf{A}}$ and ${\rm div}\,\hat{\mathbf{E}}=-m_t^2\hat{A}_0/\varepsilon_\sigma$; the homogeneous Maxwell equations remain unchanged. The polarization vector is $\hat{\mathbf{P}}={\rm i}(\sigma/\omega)\hat{\mathbf{E}}$, cf. after Eq. (2.4), and the London equation ${\rm rot}\,\hat{\mathbf{j}}={\rm i}\sigma\omega\hat{\mathbf{B}}$ applies. The dispersion relations for the transversal and longitudinal modes read as in Eqs. (2.8) and (2.10), with $\varepsilon$ replaced by $\varepsilon_\sigma$ and $\varepsilon_0=\mu_{(0)}=1$.

We consider a tachyonic conductivity

$$\sigma(\omega)=\frac{{\rm i}\omega_{\rm p}^2\omega}{\omega^2-\omega_0^2+{\rm i}\gamma_0\omega}, \tag{2.14}$$

where $\omega_{\rm p}^2:=q^2n_{\rm e}/m_{\rm e}$ is the tachyonic plasma frequency, and $n_{\rm e}$ the electron density of the medium. This is based on Drude's damped oscillator model, $\ddot{\mathbf{r}}+\gamma_0\dot{\mathbf{r}}+\omega_0^2\mathbf{r}=q\mathbf{E}/m$, with $\mathbf{r}=\hat{\mathbf{r}}\,{\rm e}^{-{\rm i}\omega t}+{\rm c.c.}$, and $\mathbf{E}$ as above [14]. $\omega_0$ is the characteristic binding frequency of the electronic oscillators, $q$ the tachyonic charge, and $\gamma_0$ is the damping constant related to the tachyonic resistivity $\rho_t$ by $\gamma_0=\omega_p^2\rho_t$. We solve this equation in dipole approximation, neglecting the spatial dependence of the Fourier components $\hat{\mathbf{E}}(\mathbf{x},\omega)$, so that $\sigma(\omega)$ in Eq. (2.14) follows from $\mathbf{j}=qn_{\rm e}\dot{\mathbf{r}}$, $\hat{\mathbf{j}}=qn_{\rm e}\hat{\mathbf{v}}$, and $\hat{\mathbf{v}}=-{\rm i}\omega\hat{\mathbf{r}}$. We note $\omega_{\rm p}^2=\omega_{\rm p,em}^2\alpha_{\rm q}/\alpha_{\rm e}$, where $\omega_{\rm p,em}^2$ is the electromagnetic plasma frequency, and $\alpha_{\rm q}/\alpha_{\rm e}\approx 1.4\times10^{-11}$ the ratio of tachyonic and electric fine structure constants. In the Heaviside–Lorentz system, $\alpha_{\rm e}=e^2/(4\pi\hbar c)\approx 1/137$ and $\alpha_{\rm q}=q^2/(4\pi\hbar c)\approx 1.0\times10^{-13}$. The tachyon–electron mass ratio is $m_t/m\approx 1/238$; $\alpha_{\rm q}$ and $m_t$ are estimated from hydrogenic Lamb shifts [6]. We may thus conclude that the tachyonic conductivity $\propto\omega_{\rm p}^2$ is by a factor of $10^{-11}$ smaller than the electric counterpart. However, $\varepsilon_\sigma(\omega)-1$ can still be of order one.

To demonstrate this, we consider a free electron gas, $\omega_0=\gamma_0=0$, so that the tachyonic conductivity (2.14) simplifies to $\sigma={\rm i}\omega_{\rm p}^2/\omega$, and the induced permittivity is $\varepsilon_\sigma=1-\omega_{\rm p}^2/\omega^2$. We may write the electromagnetic plasma frequency as $\omega_{\rm p,em}^2=4\pi c^2\lambda\!\!\!^{-}_{\rm e}\alpha_{\rm e}n_{\rm e}$, where $\lambda\!\!\!^{-}_{\rm e}$ is the reduced electronic Compton wavelength, $\alpha_{\rm e}$ the electric fine structure constant, and $n_{\rm e}$ the electron density as above. We thus find $\hbar\omega_{\rm p,em}\,[{\rm eV}]\approx 3.713\times10^{-11}n_{\rm e}^{1/2}\,[{\rm cm}^{-3}]$, and the tachyonic counterpart $\omega_{\rm p}\approx 3.74\times10^{-6}\omega_{\rm p,em}$. Metallic electron densities of $10^{22}$–$10^{23}\,{\rm cm}^{-3}$ result in a tachyonic plasma frequency $\omega_{\rm p}$ in the $10^{-5}\,{\rm eV}$ range. Thus, even though the tachyonic conductivity is much smaller than the electromagnetic one at the same frequency, the tachyonic permittivity $\varepsilon_\sigma(\omega)$ becomes noticeably different from 1 for frequencies comparable to $\omega_{\rm p}$. Finally, small frequencies of the order of $10^{-5}\,{\rm eV}$ do not imply large wavelengths. The tachyonic wavelength is $\lambda_{\rm T,L}=2\pi/k_{\rm T,L}$, with wave numbers defined in Eqs. (2.8) and (2.10). The maximal transversal/longitudinal wavelength in the medium is thus $\lambda_{\rm T}\sim\sqrt{\mu_0/\mu}\lambda_t$ and $\lambda_{\rm L}\sim\sqrt{\varepsilon/\varepsilon_0}\lambda_t$, attained in the zero frequency limit, where the permeabilities are of order one and $\lambda_t=2\pi/m_t\approx 5.8\,{\rm Å}$ is the tachyonic Compton wavelength.

## 3. Superluminal wave fields at the surface of discontinuity of dielectrics and conductors

To study tachyon refraction at the interface of two media with different permeabilities, we have to specify the boundary conditions. To this end, we split the wave fields into regular and singular parts, writing the scalar induction and the magnetic field strength as

$$\hat{C}_0=\hat{C}_{0,{\rm reg}}+\hat{C}_{0,{\rm sing}},\quad \hat{C}_{0,{\rm reg}}=\theta(S)\hat{C}_{0,2}+\theta(-S)\hat{C}_{0,1},$$
$$\hat{\mathbf{B}}=\hat{\mathbf{B}}_{\rm reg}+\hat{\mathbf{B}}_{\rm sing},\quad \hat{\mathbf{B}}_{\rm reg}=\theta(S)\hat{\mathbf{B}}_2+\theta(-S)\hat{\mathbf{B}}_1. \tag{3.1}$$

The same decomposition is used for the scalar and vector potentials $(\hat{A}_0,\hat{\mathbf{A}})$, the electric field strength $\hat{\mathbf{E}}$, and the vectorial inductions $\hat{\mathbf{C}}$, $\hat{\mathbf{D}}$, and $\hat{\mathbf{H}}$. Here, $\theta(S)$ is the Heaviside step function, and $S(\mathbf{x})=0$ is the surface separating the media defined by permeabilities $(\varepsilon_{0,1},\varepsilon_1,\mu_{0,1},\mu_1)$ and $(\varepsilon_{0,2},\varepsilon_2,\mu_{0,2},\mu_2)$, cf. Eq. (2.3), which can be frequency dependent (dispersive) and complex (dissipative). The subscripts 1 and 2 on the fields and

permeabilities refer to the respective media; in the decomposition (3.1) of the regular field components, it is understood that domain $S(\mathbf{x})>0$ is occupied by medium 2, so that $\hat{\mathbf{D}}_2=\varepsilon_2\hat{\mathbf{E}}_2$ for $S>0$, and $\hat{\mathbf{D}}_1=\varepsilon_1\hat{\mathbf{E}}_1$ applies in domain $S<0$ where medium 1 is located. The normal vector, $\mathbf{n}:=\nabla S/|\nabla S|$, thus points into the interior of medium 2. The singular part of the field, if any, is a distribution supported on the boundary surface $S=0$, typically containing a Dirac function $\delta(S)$ as factor. In contrast to the regular components in Eq. (3.1), the singular field strengths and inductions do not show in the material equations (2.3). In Sections 3.1 and 3.2, we assume vanishing charge and current densities in the field equations, as well as the absence of a singular surface current at the interface. In Section 3.3, we consider inhomogeneous boundary conditions consistent with currents.

### 3.1. Boundary conditions for transversal tachyons

We start by substituting ansatz (3.1) into the field equations (2.2) (with zero current and charge density) and the Lorentz condition, and assume that the fields subjected to rotors and divergences have no singular part. That is, we try to solve under the condition that $\hat{\mathbf{E}}$, $\hat{\mathbf{B}}$, $\hat{\mathbf{D}}$, $\hat{\mathbf{H}}$, and $\hat{\mathbf{C}}$ are regular at the interface, obtaining five relations to be satisfied at the boundary $S=0$,

$$|\nabla S|\delta(S)\mathbf{n}\cdot(\hat{\mathbf{D}}_2-\hat{\mathbf{D}}_1)=-m_{\mathrm{t}}^2\hat{C}_{0,\mathrm{sing}}, \tag{3.2}$$

$$\mathbf{n}\cdot(\hat{\mathbf{B}}_2-\hat{\mathbf{B}}_1)=0,\quad \mathbf{n}\times(\hat{\mathbf{E}}_2-\hat{\mathbf{E}}_1)=0,\quad \mathbf{n}\times(\hat{\mathbf{H}}_2-\hat{\mathbf{H}}_1)=0, \tag{3.3}$$

$$|\nabla S|\delta(S)\mathbf{n}\cdot(\hat{\mathbf{C}}_2-\hat{\mathbf{C}}_1)=-\mathrm{i}\omega\hat{C}_{0,\mathrm{sing}}, \tag{3.4}$$

where Eqs. (3.2) and (3.4) can be combined to give

$$\mathrm{i}\omega\mathbf{n}(\hat{\mathbf{D}}_2-\hat{\mathbf{D}}_1)=m_{\mathrm{t}}^2\mathbf{n}(\hat{\mathbf{C}}_2-\hat{\mathbf{C}}_1). \tag{3.5}$$

Assuming the potentials $\hat{A}_0$ and $\hat{\mathbf{A}}$ to be non-singular, we find, from the potential representation of $\hat{\mathbf{B}}$ and $\hat{\mathbf{E}}$, cf. after Eq. (2.3),

$$\mathbf{n}\times(\hat{\mathbf{A}}_2-\hat{\mathbf{A}}_1)=0,\quad \hat{A}_{0,2}-\hat{A}_{0,1}=0. \tag{3.6}$$

All fields are regular at the boundary surface, with exception of $\hat{C}_0$, whose singular part is obtained from (3.2) or (3.4). $\hat{C}_{0,\mathrm{sing}}$ does not vanish except for a special polarization (TE waves), but no singular contribution can occur in the transversal flux vector (2.12), as $\hat{A}_0$ is identically zero in both media, cf. Eq. (2.9). The boundary conditions on transversal modes are defined by Eqs. (3.3), (3.5), and (3.6).

### 3.2. Longitudinal modes generating singular magnetic field strengths at the interface

We proceed analogously to the transversal case, but now assuming all fields to be regular at the boundary except for the magnetic field $\hat{\mathbf{B}}$. On substituting ansatz (3.1) into the field equations (2.2) and (2.3) and the Lorentz condition, cf. after Eq. (2.4), we find

$$\mathbf{n}\cdot(\hat{\mathbf{D}}_2-\hat{\mathbf{D}}_1)=0,\quad \mathbf{n}\cdot(\hat{\mathbf{C}}_2-\hat{\mathbf{C}}_1)=0,\quad \mathbf{n}\times(\hat{\mathbf{H}}_2-\hat{\mathbf{H}}_1)=0, \tag{3.7}$$

$$|\nabla S|\delta(S)\mathbf{n}\times(\hat{\mathbf{E}}_2-\hat{\mathbf{E}}_1)=\mathrm{i}\omega\hat{\mathbf{B}}_{\mathrm{sing}}. \tag{3.8}$$

The potential representations of $\hat{\mathbf{B}}$ and $\hat{\mathbf{E}}$ give

$$|\nabla S|\delta(S)\mathbf{n}\times(\hat{\mathbf{A}}_2-\hat{\mathbf{A}}_1)=\hat{\mathbf{B}}_{\mathrm{sing}}, \tag{3.9}$$

$$\hat{A}_{0,2}-\hat{A}_{0,1}=0. \tag{3.10}$$

By combining Eqs. (3.8) and (3.9), we obtain

$$\mathbf{n}\times(\hat{\mathbf{E}}_2-\hat{\mathbf{E}}_1)=\mathrm{i}\omega\mathbf{n}\times(\hat{\mathbf{A}}_2-\hat{\mathbf{A}}_1). \tag{3.11}$$

Finally, the divergence equation, $\mathrm{div}(\hat{\mathbf{B}}_{\mathrm{reg}}+\hat{\mathbf{B}}_{\mathrm{sing}})=0$, results in

$$\mathbf{n}(\hat{\mathbf{B}}_2-\hat{\mathbf{B}}_1)=0, \tag{3.12}$$

where we used (3.9). Eqs. (3.7) and (3.10)–(3.12) constitute the boundary conditions for longitudinal modes. The regular longitudinal $\hat{\mathbf{B}}$ field vanishes identically in both media, cf. Eq. (2.11), but a singular surface field $\hat{\mathbf{B}}_{\mathrm{sing}}$ emerges, which, however, does not affect the longitudinal flux vector (2.12), since all other field strengths, potentials, and inductions are regular.

The transversal and longitudinal boundary conditions derived in Sections 3.1 and 3.2 apply at the interface of two media with different permeabilities discontinuous at the interface. They unambiguously determine the refractive properties of tachyons, such as deflection and reflection angles, and assure transmission and reflection ratios consistent with energy conservation in non-absorptive media, cf. Section 4.

### 3.3. Singular boundary currents and charge densities

In the case of non-vanishing charge and current densities in field equations (2.2), the transversal and longitudinal boundary conditions derived in Sections 3.1 and 3.2 become inhomogeneous due to singular surface currents. As in (3.1), we split current and charge density into a regular and singular part,

$$\hat{\rho}=\hat{\rho}_{\mathrm{reg}}+\hat{\rho}_{\mathrm{sing}},\quad \hat{\rho}_{\mathrm{reg}}=\theta(S)\hat{\rho}_2+\theta(-S)\hat{\rho}_1,$$

$$\hat{\mathbf{j}}=\hat{\mathbf{j}}_{\mathrm{reg}}+\hat{\mathbf{j}}_{\mathrm{sing}},\quad \hat{\mathbf{j}}_{\mathrm{reg}}=\theta(S)\hat{\mathbf{j}}_2+\theta(-S)\hat{\mathbf{j}}_1. \tag{3.13}$$

The singular surface charge and current, $\hat{\rho}_{\mathrm{sing}}$ and $\hat{\mathbf{j}}_{\mathrm{sing}}$, are supported at the interface $S=0$. The subscripts 1 and 2 refer to the respective medium as defined after Eq. (3.1). We substitute ansatz (3.13) into the continuity equation, cf. after Eq. (2.4), to find the boundary condition required by current conservation,

$$|\nabla S|\delta(S)\mathbf{n}\cdot(\hat{\mathbf{j}}_2-\hat{\mathbf{j}}_1)=\mathrm{i}\omega\hat{\rho}_{\mathrm{sing}}-\mathrm{div}\hat{\mathbf{j}}_{\mathrm{sing}}. \tag{3.14}$$

Three of the transversal boundary conditions in Section 3.1 have to be modified in the presence of currents. Condition (3.2) is replaced by

$$|\nabla S|\delta(S)\mathbf{n}\cdot(\hat{\mathbf{D}}_2-\hat{\mathbf{D}}_1)=\hat{\rho}_{\mathrm{sing}}-m_{\mathrm{t}}^2\hat{C}_{0,\mathrm{sing}}, \tag{3.15}$$

the third condition in Eq. (3.3) reads

$$|\nabla S|\delta(S)\mathbf{n}\times(\hat{\mathbf{H}}_2-\hat{\mathbf{H}}_1)=\hat{\mathbf{j}}_{\mathrm{sing}}, \tag{3.16}$$

and condition (3.5) becomes inhomogeneous as well:

$$|\nabla S|\delta(S)(\mathrm{i}\omega\mathbf{n}(\hat{\mathbf{D}}_2-\hat{\mathbf{D}}_1)-m_{\mathrm{t}}^2\mathbf{n}(\hat{\mathbf{C}}_2-\hat{\mathbf{C}}_1))=\mathrm{i}\omega\hat{\rho}_{\mathrm{sing}}. \tag{3.17}$$

As for the longitudinal boundary conditions in Section 3.2, there are two changes. The first condition in Eq. (3.7) is replaced by Eq. (3.15) with $\hat{C}_{0,\mathrm{sing}}=0$, and the third condition in Eq. (3.7) by Eq. (3.16). It is easy to check that boundary condition (3.16) is consistent with current conservation (3.14).

## 4. Tachyon refraction at plane interfaces of dispersive media

We take the $z=0$ plane as the interface $S$ separating medium 2 in the upper half-space $z>0$ from medium 1 in the lower half-space. The media are defined by frequency-dependent permeabilities $(\varepsilon_{0,1},\varepsilon_1,\mu_{0,1},\mu_1)$ and $(\varepsilon_{0,2},\varepsilon_2,\mu_{0,2},\mu_2)$, respectively, cf. Eq. (2.3) and after Eq. (3.1). We consider a tachyonic plane wave, cf. after Eq. (2.7), incident from the lower half-space upon the interface, the $\mathbf{e}_{1,2}$ plane. The wave number $k_{\mathrm{in}}$ of this incoming transversal or longitudinal wave is defined by dispersion relation (2.8) or (2.10), with permeabilities carrying subscript 1. Part of the wave is reflected back into medium 1, and the wave number $k_{\mathrm{re}}$ of

the reflected wave coincides with $k_{\rm in}$. The wave number $k_{\rm tr}$ of the wave transmitted into the upper half-space is determined by the permeabilities of medium 2. The wave vectors of the respective modes are denoted by $\mathbf{k}_{\rm in}=k_{\rm in}\mathbf{k}_{0,\rm in}$, $\mathbf{k}_{\rm re}=k_{\rm re}\mathbf{k}_{0,\rm re}$, and $\mathbf{k}_{\rm tr}=k_{\rm tr}\mathbf{k}_{0,\rm tr}$, where the zero subscript indicates unit vectors. We assume the incoming plane wave to be homogeneous, so that $\mathbf{k}_{0,\rm in}$ is a real unit vector; the wave numbers $k_{\rm in,tr}$ can be complex. Since $\mathbf{k}_{0,\rm in}$ is real, the unit wave vector $\mathbf{k}_{0,\rm re}$ of the reflected wave is real too, as shown below. The transmitted wave is in general inhomogeneous if the wave number in medium 1 or 2 is complex, so that $\mathbf{k}_{0,\rm tr}$ is a complex unit vector, $\mathbf{k}_{0,\rm tr}^2=1$. We adopt the convention $\mathrm{Re}(k_{\rm in,tr})>0$, since wave numbers are only defined as squares by the dispersion relations. If medium 1 in the lower half-space has real permeabilities, the vacuum for instance, then the incident wave number $k_{\rm in}$ is real.

We choose the incoming real unit wave vector $\mathbf{k}_{0,\rm in}$ in the $\mathbf{e}_{1,3}$ plane. (The $\mathbf{e}_i$ are coordinate unit vectors.) The normal vector of the interface is $\mathbf{e}_3$, pointing into medium 2. A convenient angular parametrization of the wave vectors is

$$\begin{aligned}&\sin\theta_{\rm in}=\mathbf{k}_{0,\rm in}\cdot\mathbf{e}_1,\quad \sin\theta_{\rm re}=\mathbf{k}_{0,\rm re}\cdot\mathbf{e}_1,\quad \sin\theta_{\rm tr}=\mathbf{k}_{0,\rm tr}\cdot\mathbf{e}_1\\ &\cos\theta_{\rm in}=\mathbf{k}_{0,\rm in}\cdot\mathbf{e}_3,\quad \cos\theta_{\rm re}=\mathbf{k}_{0,\rm re}\cdot\mathbf{e}_3,\quad \cos\theta_{\rm tr}=\mathbf{k}_{0,\rm tr}\cdot\mathbf{e}_3.\end{aligned}\tag{4.1}$$

The incoming wave moves through the lower half-space towards the interface at $z=0$, so that $\cos\theta_{\rm in}$ and $\sin\theta_{\rm in}$ are positive, $k_{\rm in}=k_{\rm re}$, $\cos\theta_{\rm re}=-\cos\theta_{\rm in}$, and $\sin\theta_{\rm re}=\sin\theta_{\rm in}$. The angles $\cos\theta_{\rm tr}$ and $\sin\theta_{\rm tr}$ in Eq. (4.1) are in general complex, and $\theta_{\rm re}=\pi-\theta_{\rm in}$. The boundary conditions at $z=0$ can only be satisfied if the phase factors $\mathrm{e}^{\mathrm{i}\mathbf{k}\cdot\mathbf{x}}$ of the three waves coincide at the boundary. This requires $\mathbf{k}_{\rm in}\cdot\mathbf{e}_1=\mathbf{k}_{\rm re}\cdot\mathbf{e}_1=\mathbf{k}_{\rm tr}\cdot\mathbf{e}_1$, and the same for $\mathbf{e}_2$ at the interface. (The wave vectors are orthogonal to $\mathbf{e}_2$, as $\mathbf{k}_{0,\rm in}$ is by definition.) Hence, $k_{\rm in}\sin\theta_{\rm in}=k_{\rm re}\sin\theta_{\rm re}=k_{\rm tr}\sin\theta_{\rm tr}$, which is the tachyonic counterpart to Snell's reflection law [19,20].

The refractive indices of medium 1 and 2 are denoted by $n_{1,2}=k_{\rm in,tr}/\omega$, cf. Eq. (2.13), and their ratio by $\hat n=n_2/n_1$. This applies to transversal as well as longitudinal indices, e.g., $\hat n_{\rm T}=n_{\rm T,2}/n_{\rm T,1}$. The transversal/longitudinal refraction law can thus be written as $\sin\theta_{\rm in}/\sin\theta_{\rm tr}=\hat n_{\rm T,L}$. In the high-frequency regime $\omega\gg m_t$, the transversal refractive index ratio simplifies to $\hat n_{\rm T}\sim\sqrt{\varepsilon_2\mu_2/(\varepsilon_1\mu_1)}$, and the longitudinal one to $\hat n_{\rm L}\sim\sqrt{\varepsilon_{0,2}\mu_{0,2}/(\varepsilon_{0,1}\mu_{0,1})}$, cf. after Eq. (2.13). In the low-frequency limit, $\omega\ll m_t$, the refraction angle $\theta_{\rm tr}$ is determined by $\hat n_{\rm T}\sim\sqrt{\mu_2\mu_{0,1}/(\mu_1\mu_{0,2})}$ or $\hat n_{\rm L}\sim\sqrt{\varepsilon_1\varepsilon_{0,2}/(\varepsilon_2\varepsilon_{0,1})}$. If we consider dielectrics with $\mu_{(0)}=\varepsilon_0=1$, the longitudinal refractive index ratio $\hat n_{\rm L}\sim\sqrt{\varepsilon_1/\varepsilon_2}$ at low frequencies is just the inverse of $\hat n_{\rm T}$ at high frequency. The refraction law can thus be used to discriminate between transversal and longitudinal polarization.

### 4.1. Refraction of superluminal TE and TM waves

We first consider tachyonic TE waves, so that the incoming mode $\hat{\mathbf{E}}_{\rm in}$ is linearly polarized, with amplitude orthogonal to the plane of incidence generated by the normal vector $\mathbf{e}_3$ of the boundary and the wave vector $\mathbf{k}_{0,\rm in}$ in the $\mathbf{e}_{1,3}$ plane. Thus, $\hat{\mathbf{E}}_{\rm in}=E_{\rm in}\mathbf{e}_2\mathrm{e}^{\mathrm{i}\mathbf{k}_{\rm in}\cdot\mathbf{x}}$, cf. Eq. (2.9). The boundary conditions stated in Section 3.1 are satisfied by the reflected and transmitted waves, which are likewise polarized in the $\mathbf{e}_2$ direction, so that the respective modes are $E_{\rm re}\mathbf{e}_2\mathrm{e}^{\mathrm{i}\mathbf{k}_{\rm re}\cdot\mathbf{x}}$ and $E_{\rm tr}\mathbf{e}_2\mathrm{e}^{\mathrm{i}\mathbf{k}_{\rm tr}\cdot\mathbf{x}}$. The wave numbers of the incident and reflected waves are defined by the transversal dispersion relation (2.8) of medium 1 with permeabilities $(\varepsilon_{0,1},\varepsilon_1,\mu_{0,1},\mu_1)$, cf. Eq. (2.3). The wave number of the transmitted wave is calculated with the permeabilities $(\varepsilon_{0,2},\varepsilon_2,\mu_{0,2},\mu_2)$ of medium 2 in the upper half-space. The boundary conditions (3.3), (3.5) and (3.6) give, if combined with Snell's law as stated above, two independent relations for the three amplitudes:

$$\begin{aligned}&E_{\rm in}+E_{\rm re}-E_{\rm tr}=0,\\ &\frac{k_{\rm in}}{\mu_1}E_{\rm in}\cos\theta_{\rm in}+\frac{k_{\rm re}}{\mu_1}E_{\rm re}\cos\theta_{\rm re}-\frac{k_{\rm tr}}{\mu_2}E_{\rm tr}\cos\theta_{\rm tr}=0,\end{aligned}\tag{4.2}$$

obtained via $\mathbf{n}\times(\hat{\mathbf{E}}_2-\hat{\mathbf{E}}_1)=0$ and $\mathbf{n}\times(\hat{\mathbf{H}}_2-\hat{\mathbf{H}}_1)=0$. We write this in amplitude ratios by means of Eq. (4.1):

$$\begin{aligned}\frac{E_{\rm re}}{E_{\rm in}}&=\frac{\mu_2k_{\rm in}\cos\theta_{\rm in}-\mu_1k_{\rm tr}\cos\theta_{\rm tr}}{\mu_2k_{\rm in}\cos\theta_{\rm in}+\mu_1k_{\rm tr}\cos\theta_{\rm tr}},\\ \frac{E_{\rm tr}}{E_{\rm in}}&=\frac{2\mu_2k_{\rm in}\cos\theta_{\rm in}}{\mu_2k_{\rm in}\cos\theta_{\rm in}+\mu_1k_{\rm tr}\cos\theta_{\rm tr}}.\end{aligned}\tag{4.3}$$

Using Snell's law, we parametrize by the incidence angle, substituting $\cos\theta_{\rm tr}=\sqrt{1-(k_{\rm in}/k_{\rm tr})^2\sin^2\theta_{\rm in}}$. Even though we employ here and in the following only two boundary conditions, the remaining ones are satisfied as well, by virtue of the above refraction laws.

We turn to superluminal TM waves, where the electric field is linearly polarized parallel to the plane of incidence. It is convenient to write the boundary conditions in terms of the magnetic field, by way of $\hat{\mathbf{E}}=-(\mu\omega/k)\mathbf{k}_0\times\hat{\mathbf{H}}$, where $\hat{\mathbf{H}}$ is orthogonal to the plane of incidence, cf. Eq. (2.9). Accordingly, $\hat{\mathbf{H}}_{\rm in}=H_{\rm in}\mathbf{e}_2\,\mathrm{e}^{\mathrm{i}\mathbf{k}_{\rm in}\cdot\mathbf{x}}$, and analogously for the reflected and transmitted modes. The boundary conditions for transversal modes again give two independent relations among the three amplitudes,

$$\begin{aligned}&H_{\rm in}+H_{\rm re}-H_{\rm tr}=0,\\ &\frac{\mu_1}{k_{\rm in}}H_{\rm in}\cos\theta_{\rm in}+\frac{\mu_1}{k_{\rm re}}H_{\rm re}\cos\theta_{\rm re}-\frac{\mu_2}{k_{\rm tr}}H_{\rm tr}\cos\theta_{\rm tr}=0.\end{aligned}\tag{4.4}$$

Here, we used the same two boundary conditions as for TE modes. The amplitude ratios read

$$\begin{aligned}\frac{H_{\rm re}}{H_{\rm in}}&=\frac{\mu_1k_{\rm tr}\cos\theta_{\rm in}-\mu_2k_{\rm in}\cos\theta_{\rm tr}}{\mu_1k_{\rm tr}\cos\theta_{\rm in}+\mu_2k_{\rm in}\cos\theta_{\rm tr}},\\ \frac{H_{\rm tr}}{H_{\rm in}}&=\frac{2\mu_1k_{\rm tr}\cos\theta_{\rm in}}{\mu_1k_{\rm tr}\cos\theta_{\rm in}+\mu_2k_{\rm in}\cos\theta_{\rm tr}},\end{aligned}\tag{4.5}$$

which differ from the TE ratios just by an interchange of $\mu_1k_{\rm tr}$ and $\mu_2k_{\rm in}$, and we substitute $\cos\theta_{\rm tr}$ stated after Eq. (4.3) to parametrize by the incidence angle.

The energy flux (i.e., the incident, reflected, or transmitted energy per unit time and unit surface area) carried by a superluminal mode with real unit wave vector $\mathbf{k}_0$ is $F^{\rm T,L}:=|\langle\mathbf{S}^{\rm T,L}\rangle||\mathbf{k}_0\cdot\mathbf{n}|$. The transversal and longitudinal flux vectors $\langle\mathbf{S}^{\rm T,L}\rangle$ are defined in Eq. (2.12), with the respective incident, reflected, or transmitted wave substituted. As for the transmitted wave, we assume the two media to be non-dissipative, so that $\mathbf{k}_{0,\rm tr}$ is real. The superscripts T and L denote transversal and longitudinal waves, the latter are studied in Section 4.2. The transversal and longitudinal reflection and transmission coefficients are defined by the flux ratios

$$R^{\rm T,L}:=\frac{F^{\rm T,L}_{\rm re}}{F^{\rm T,L}_{\rm in}}=\frac{|\langle\mathbf{S}^{\rm T,L}_{\rm re}\rangle|}{|\langle\mathbf{S}^{\rm T,L}_{\rm in}\rangle|},\quad T^{\rm T,L}:=\frac{F^{\rm T,L}_{\rm tr}}{F^{\rm T,L}_{\rm in}}=\frac{|\langle\mathbf{S}^{\rm T,L}_{\rm tr}\rangle|\cos\theta_{\rm tr}}{|\langle\mathbf{S}^{\rm T,L}_{\rm in}\rangle|\cos\theta_{\rm in}},\tag{4.6}$$

where the subscripts indicate the respective fields (incident, reflected, or transmitted) to be substituted into the flux vector. Energy conservation requires $R^{\rm T,L}+T^{\rm T,L}=1$. (We do not define a transmission coefficient for dissipative media.) By making use of the transversal flux vector (2.12), we find the reflection and

transmission ratios of tachyonic TE and TM modes as

$$R^{\mathrm{T}}_{\mathrm{TE}}=|E_{\mathrm{re}}/E_{\mathrm{in}}|^2,\quad R^{\mathrm{T}}_{\mathrm{TM}}=|H_{\mathrm{re}}/H_{\mathrm{in}}|^2,$$
$$T^{\mathrm{T}}_{\mathrm{TE}}=\frac{\mu_1 k_{\mathrm{tr}}|E_{\mathrm{tr}}|^2\cos\,\theta_{\mathrm{tr}}}{\mu_2 k_{\mathrm{in}}|E_{\mathrm{in}}|^2\cos\,\theta_{\mathrm{in}}},\quad T^{\mathrm{T}}_{\mathrm{TM}}=\frac{\mu_2 k_{\mathrm{in}}|H_{\mathrm{tr}}|^2\cos\,\theta_{\mathrm{tr}}}{\mu_1 k_{\mathrm{tr}}|H_{\mathrm{in}}|^2\cos\,\theta_{\mathrm{in}}},\tag{4.7}$$

with the amplitude ratios (4.3) and (4.5) substituted. It is easy to check that energy is conserved, which suggests that we have got the boundary conditions in Section 3.1 right.

At normal incidence, $\theta_{\mathrm{in}}=\theta_{\mathrm{tr}}=0$, $\theta_{\mathrm{re}}=\pi$, the amplitude ratios (4.3) and (4.5) reduce to

$$\frac{E_{\mathrm{re}}}{E_{\mathrm{in}}}=\frac{\hat\mu\hat n_{\mathrm{T}}-1}{\hat\mu\hat n_{\mathrm{T}}+1},\quad \frac{E_{\mathrm{tr}}}{E_{\mathrm{in}}}=\frac{2\hat\mu}{\hat\mu\hat n_{\mathrm{T}}+1},\quad \frac{H_{\mathrm{re}}}{H_{\mathrm{in}}}=\frac{\hat n_{\mathrm{T}}-\hat\mu}{\hat n_{\mathrm{T}}+\hat\mu},\quad \frac{H_{\mathrm{tr}}}{H_{\mathrm{in}}}=\frac{2\hat n_{\mathrm{T}}}{\hat n_{\mathrm{T}}+\hat\mu},\tag{4.8}$$

where $\hat n_{\mathrm{T}}=n_{\mathrm{T},2}/n_{\mathrm{T},1}$ is the ratio of the transversal refractive indices of medium 1 and 2, and $\hat\mu=\mu_2/\mu_1$, cf. after Eq. (4.1). In the high-frequency regime $\omega\gg m_{\mathrm{t}}$, we approximate $n_{\mathrm{T}}\sim\sqrt{\varepsilon\mu}$, cf. after Eq. (2.13), and find the reflection coefficients for TE and TM waves as

$$R^{\mathrm{T}}_{\mathrm{TE}}\sim\left(\frac{\sqrt{\varepsilon_2\mu_2^3}-\sqrt{\varepsilon_1\mu_1^3}}{\sqrt{\varepsilon_2\mu_2^3}+\sqrt{\varepsilon_1\mu_1^3}}\right)^2,\quad R^{\mathrm{T}}_{\mathrm{TM}}\sim\left(\frac{\sqrt{\varepsilon_2\mu_1}-\sqrt{\varepsilon_1\mu_2}}{\sqrt{\varepsilon_2\mu_1}+\sqrt{\varepsilon_1\mu_2}}\right)^2.\tag{4.9}$$

At low frequency $\omega\ll m_{\mathrm{t}}$, we substitute $n_{\mathrm{T}}\sim\sqrt{\mu/\mu_0}m_{\mathrm{t}}/\omega$ in Eq. (4.8):

$$R^{\mathrm{T}}_{\mathrm{TE}}\sim\left(\frac{\sqrt{\mu_{0,1}\mu_2^3}-\sqrt{\mu_{0,2}\mu_1^3}}{\sqrt{\mu_{0,1}\mu_2^3}+\sqrt{\mu_{0,2}\mu_1^3}}\right)^2,\quad R^{\mathrm{T}}_{\mathrm{TM}}\sim\left(\frac{\sqrt{\mu_{0,1}\mu_1}-\sqrt{\mu_{0,2}\mu_2}}{\sqrt{\mu_{0,1}\mu_1}+\sqrt{\mu_{0,2}\mu_2}}\right)^2.\tag{4.10}$$

In this limit, the reflected fraction of the transversal tachyon flux is determined by the magnetic permeabilities only. Transversal refraction will further be discussed after Eq. (4.16), together with the longitudinal reflection coefficients derived in Section 4.2.

### 4.2. Manifestations of the negative mass-square: longitudinal refraction, Brewster angles, and total internal reflection

We start with a longitudinal incident mode, $\hat{\mathbf{E}}_{\mathrm{in}}=E_{\mathrm{in}}\mathbf{k}_{0,\mathrm{in}}\,\mathrm{e}^{\mathrm{i}\mathbf{k}_{\mathrm{in}}\cdot\mathbf{x}}$, and use analogous notation for the reflected and transmitted fields. All wave vectors lie in the $\mathbf{e}_{1,3}$ plane. The permeabilities of media 1 and 2 are labeled as indicated before Eq. (4.2). The boundary conditions (3.7) and (3.10)–(3.12) give two independent relations for the amplitudes,

$$\frac{\varepsilon_1}{\varepsilon_{0,1}}k_{\mathrm{in}}E_{\mathrm{in}}+\frac{\varepsilon_1}{\varepsilon_{0,1}}k_{\mathrm{re}}E_{\mathrm{re}}-\frac{\varepsilon_2}{\varepsilon_{0,2}}k_{\mathrm{tr}}E_{\mathrm{tr}}=0,$$
$$\varepsilon_1E_{\mathrm{in}}\,\cos\,\theta_{\mathrm{in}}+\varepsilon_1E_{\mathrm{re}}\,\cos\,\theta_{\mathrm{re}}-\varepsilon_2E_{\mathrm{tr}}\,\cos\,\theta_{\mathrm{tr}}=0,\tag{4.11}$$

derived from $\hat A_{0,2}-\hat A_{0,1}=0$ and $\mathbf{n}(\hat{\mathbf{C}}_2-\hat{\mathbf{C}}_1)=0$. The amplitude ratios read accordingly

$$\frac{E_{\mathrm{re}}}{E_{\mathrm{in}}}=\frac{\varepsilon_{0,1}k_{\mathrm{tr}}\,\cos\,\theta_{\mathrm{in}}-\varepsilon_{0,2}k_{\mathrm{in}}\,\cos\,\theta_{\mathrm{tr}}}{\varepsilon_{0,1}k_{\mathrm{tr}}\,\cos\,\theta_{\mathrm{in}}+\varepsilon_{0,2}k_{\mathrm{in}}\,\cos\,\theta_{\mathrm{tr}}},$$
$$\frac{E_{\mathrm{tr}}}{E_{\mathrm{in}}}=\frac{\varepsilon_1}{\varepsilon_2}\frac{2\varepsilon_{0,2}k_{\mathrm{in}}\,\cos\,\theta_{\mathrm{in}}}{\varepsilon_{0,1}k_{\mathrm{tr}}\,\cos\,\theta_{\mathrm{in}}+\varepsilon_{0,2}k_{\mathrm{in}}\,\cos\,\theta_{\mathrm{tr}}},\tag{4.12}$$

with $\cos\,\theta_{\mathrm{tr}}$ defined after Eq. (4.3). The singular surface magnetic field $\hat{\mathbf{B}}_{\mathrm{sing}}$ is calculated via Eq. (3.9):

$$\hat{\mathbf{B}}_{\mathrm{sing}}=\mathbf{e}_2\delta(z)\frac{\mathrm{i}\omega}{m_t^2}E_{\mathrm{in}}\,\sin\,\theta_{\mathrm{in}}\left(\frac{E_{\mathrm{tr}}}{E_{\mathrm{in}}}\frac{k_{\mathrm{in}}}{k_{\mathrm{tr}}}\varepsilon_2\mu_{0,2}-\left(1+\frac{E_{\mathrm{re}}}{E_{\mathrm{in}}}\right)\varepsilon_1\mu_{0,1}\right).\tag{4.13}$$

The longitudinal reflection and transmission coefficients defined in Eqs. (2.12) and (4.6) are

$$R^{\mathrm{L}}=\frac{|E_{\mathrm{re}}|^2}{|E_{\mathrm{in}}|^2},\quad T^{\mathrm{L}}=\frac{\varepsilon_2^2}{\varepsilon_1^2}\frac{\varepsilon_{0,1}}{\varepsilon_{0,2}}\frac{k_{\mathrm{tr}}}{k_{\mathrm{in}}}\frac{|E_{\mathrm{tr}}|^2}{|E_{\mathrm{in}}|^2}\frac{\cos\,\theta_{\mathrm{tr}}}{\cos\,\theta_{\mathrm{in}}},\tag{4.14}$$

where we substitute the ratios (4.12). The transmission coefficient applies for real permeabilities, energy being conserved in non-absorptive media, $R^{\mathrm{L}}+T^{\mathrm{L}}=1$.

At normal incidence, $\theta_{\mathrm{in}}=\theta_{\mathrm{tr}}=0$, the ratios (4.12) simplify,

$$\frac{E_{\mathrm{re}}}{E_{\mathrm{in}}}=\frac{\hat n_{\mathrm{L}}-\hat\varepsilon_0}{\hat n_{\mathrm{L}}+\hat\varepsilon_0},\quad \frac{E_{\mathrm{tr}}}{E_{\mathrm{in}}}=\frac{1}{\hat\varepsilon}\frac{2\hat\varepsilon_0}{\hat n_{\mathrm{L}}+\hat\varepsilon_0},\tag{4.15}$$

where $\hat\varepsilon=\varepsilon_2/\varepsilon_1$, $\hat\varepsilon_0=\varepsilon_{0,2}/\varepsilon_{0,1}$, and $\hat n_{\mathrm{L}}$ is the quotient $n_{\mathrm{L},2}/n_{\mathrm{L},1}$ of the longitudinal refractive indices, cf. Eq. (2.13). At high frequency $\omega\gg m_{\mathrm{t}}$, we find $n_{\mathrm{L}}\sim\sqrt{\varepsilon_0\mu_0}$, and for $\omega\ll m_{\mathrm{t}}$ the refractive index becomes $n_{\mathrm{L}}\sim\sqrt{\varepsilon_0/\varepsilon}m_t/\omega$, so that the longitudinal reflection coefficients read in the respective limit

$$R^{\mathrm{L}}_{(\omega\gg m_t)}\sim\left(\frac{\sqrt{\varepsilon_{0,2}\mu_{0,1}}-\sqrt{\varepsilon_{0,1}\mu_{0,2}}}{\sqrt{\varepsilon_{0,2}\mu_{0,1}}+\sqrt{\varepsilon_{0,1}\mu_{0,2}}}\right)^2,$$
$$R^{\mathrm{L}}_{(\omega\ll m_t)}\sim\left(\frac{\sqrt{\varepsilon_{0,1}\varepsilon_1}-\sqrt{\varepsilon_{0,2}\varepsilon_2}}{\sqrt{\varepsilon_{0,1}\varepsilon_1}+\sqrt{\varepsilon_{0,2}\varepsilon_2}}\right)^2.\tag{4.16}$$

If we consider vacuum permeabilities in medium 1, $\varepsilon_{(0),1}=\mu_{(0),1}=1$, and a dielectric permeability $\varepsilon_2$ different from one in medium 2 (with $\varepsilon_{0,2}=\mu_{(0),2}=1$), we find $R^{\mathrm{L}}_{(\omega\gg m_t)}\approx0$ and a finite reflectivity, $R^{\mathrm{L}}_{(\omega\ll m_t)}\sim(1-\sqrt{\varepsilon_2})^2/(1+\sqrt{\varepsilon_2})^2$, for longitudinal modes in the low-frequency regime. The same finite reflectivity applies for tachyonic TE and TM modes, but in the opposite limit, $\omega\gg m_t$, with different $\varepsilon_2(\omega)$, cf. Eq. (4.9). The transversal reflection coefficients Eq. (4.10) valid for $\omega\ll m_t$ vanish, as the indicated leading order of the frequency expansion is independent of $\varepsilon_2$.

We consider two other special cases. First, the case where the refracted wave vector is orthogonal to the reflected wave, $\theta_{\mathrm{re}}-\theta_{\mathrm{tr}}=\pi/2$, so that $\theta_{\mathrm{tr}}+\theta_{\mathrm{in}}=\pi/2$, and thus $\cos\,\theta_{\mathrm{tr}}=\sin\,\theta_{\mathrm{in}}$ and $\cos\,\theta_{\mathrm{in}}=\sin\,\theta_{\mathrm{tr}}$. This Brewster incidence angle, $\tan\,\theta_{\mathrm{in}}=\hat n_{\mathrm{T,L}}$, follows from the refraction law stated after Eq. (4.1); $\hat n_{\mathrm{T,L}}$ denotes the transversal or longitudinal refractive index ratio, cf. after Eqs. (4.8) and (4.15). The refractive indices are assumed to be real in both media. As for TM waves, we find $H_{\mathrm{re}}=0$ in Eq. (4.5), provided that the magnetic permeabilities $\mu_1$ and $\mu_2$ of the two media coincide. Similarly for longitudinally polarized waves, $E_{\mathrm{re}}=0$ in Eq. (4.12), provided that $\varepsilon_{0,1}=\varepsilon_{0,2}$. At this incidence angle, the energy of a tachyonic TM wave or a longitudinal wave is fully transmitted. If the incident transversal wave is elliptically polarized (being a complex linear combination of TE and TM waves), the reflected wave is a TE wave linearly polarized orthogonal to the plane of incidence. If we do not require $\mu_1=\mu_2$, and define the incidence angle by $H_{\mathrm{re}}=0$, we find

$$\tan\,\theta_{\mathrm{in}}=\frac{\hat n_{\mathrm{T}}}{\hat\mu}\sqrt{\frac{\hat n_{\mathrm{T}}^2-\hat\mu^2}{\hat n_{\mathrm{T}}^2-1}}.\tag{4.17}$$

The longitudinal incidence angle defined by $E_{\mathrm{re}}=0$ is likewise given by Eq. (4.17), with $\hat\mu$ replaced by $\hat\varepsilon_0$, and $\hat n_{\mathrm{T}}$ by $\hat n_{\mathrm{L}}$, cf. Eqs. (4.8) and (4.15).

The second special case is total internal reflection, which requires real wave numbers and incidence angles satisfying $\sin\,\theta_{\mathrm{in}}\geqslant\hat n_{\mathrm{T,L}}$, so that $\cos\,\theta_{\mathrm{tr}}$ defined after Eq. (4.3) is zero or imaginary with $\mathrm{Im}(\cos\,\theta_{\mathrm{tr}})>0$ to ensure damping. (More generally, the damping condition for a transmitted wave in medium 2 is $\mathrm{Im}(k_{\mathrm{tr}}\cos\,\theta_{\mathrm{tr}})>0$.) Thus $\mathbf{k}_{0,\mathrm{tr}}$ is a complex unit vector, even though the permeabilities in both media are real; its $\mathbf{e}_1$ component $\sin\,\theta_{\mathrm{tr}}$ is found via Snell's law, cf. after Eq. (4.1). The reflection coefficients $R^{\mathrm{T,L}}$ in Eqs. (4.7) and (4.14) are equal to 1, so that the incident flux is totally reflected. The refracted wave in medium 2

is exponentially damped along the $z$ axis, and no energy is transmitted. Internal reflection can only occur if $\hat{n}_{\mathrm{T,L}} \leqslant 1$, that is, medium 1 must be optically thicker than medium 2 for transversal or longitudinal modes. A third special case, normal incidence on a boundary layer of finite thickness separating two dielectric media, is discussed in the next subsection.

### 4.3. Normal incidence: reflection and transmission of tachyons at a boundary layer

We consider three dispersive media separated by parallel boundary planes $z=0$ and $z=h$. Medium 1 lies in the lower half-space, medium 2 is a layer of thickness $h$ located in $0<z<h$, and medium 3 fills the half-space $z>h$. The respective permeabilities and refractive indices are denoted by subscripts, $\varepsilon_{1,2,3}$, etc., cf. after Eq. (3.1). The layer is hit by a tachyonic plane wave propagating in the lower half-space orthogonally incident upon the $z=0$ plane. To satisfy the boundary conditions at the two interfaces, we start with the ansatz

$$E_1 = E_{\mathrm{in}}\mathrm{e}^{\mathrm{i}k_{\mathrm{in}}z} + E_{\mathrm{re}}\,\mathrm{e}^{-\mathrm{i}k_{\mathrm{in}}z}, \quad E_2 = E_{\mathrm{tr1}}\,\mathrm{e}^{\mathrm{i}k_{\mathrm{tr}}z} + E_{\mathrm{tr2}}\,\mathrm{e}^{-\mathrm{i}k_{\mathrm{tr}}z},$$
$$E_3 = E_{\mathrm{out}}\,\mathrm{e}^{\mathrm{i}k_{\mathrm{out}}z}, \tag{4.18}$$

where the $E_i$ are fields in the respective media. The notation is explained at the beginning of Section 4 and in the previous two subsections. The transversal field strengths $\hat{\mathbf{E}}_i$ are complex linear combinations of the linearly polarized fields $E_i\mathbf{e}_1$ and $E_i\mathbf{e}_2$, and the longitudinal ones read $E_i\mathbf{e}_3$. Thus, $E_1\mathbf{e}_k$ is a superposition of the incoming and reflected waves in medium 1, the wave number in this medium being $k_{\mathrm{in}}$. Similarly, $E_2\mathbf{e}_k$ is composed of the wave transmitted into medium 2 and a second wave arising by reflection at the second interface $z=h$. Finally, $E_3\mathbf{e}_k$ is the outgoing wave in medium 3. $k_{\mathrm{tr}}$ and $k_{\mathrm{out}}$ are the wave numbers in medium 2 and 3, respectively. All wave numbers have a positive real part, so that the negative sign in the exponents of the reflected waves implies the unit wave vector $-\mathbf{e}_3$. We take the amplitude of the incident wave $E_{\mathrm{in}}$ as input parameter; the remaining four amplitudes are obtained from the boundary conditions at the two interfaces.

#### 4.3.1. Transversally polarized superluminal modes

The boundary conditions for transversal tachyons read, cf. Sections 3.1 and 4.1,

$$E_{\mathrm{in}} + E_{\mathrm{re}} = E_{\mathrm{tr1}} + E_{\mathrm{tr2}}, \quad \frac{k_{\mathrm{in}}}{\mu_1}(E_{\mathrm{in}} - E_{\mathrm{re}}) = \frac{k_{\mathrm{tr}}}{\mu_2}(E_{\mathrm{tr1}} - E_{\mathrm{tr2}}),$$

$$E_{\mathrm{tr1}}\mathrm{e}^{\mathrm{i}k_{\mathrm{tr}}h} + E_{\mathrm{tr2}}\,\mathrm{e}^{-\mathrm{i}k_{\mathrm{tr}}h} = E_{\mathrm{out}}\,\mathrm{e}^{\mathrm{i}k_{\mathrm{out}}h},$$
$$\frac{k_{\mathrm{tr}}}{\mu_2}(E_{\mathrm{tr1}}\,\mathrm{e}^{\mathrm{i}k_{\mathrm{tr}}h} - E_{\mathrm{tr2}}\,\mathrm{e}^{-\mathrm{i}k_{\mathrm{tr}}h}) = \frac{k_{\mathrm{out}}}{\mu_3}E_{\mathrm{out}}\,\mathrm{e}^{\mathrm{i}k_{\mathrm{out}}h}. \tag{4.19}$$

The third and fourth of these equations lead to the amplitude ratios

$$\frac{E_{\mathrm{tr2}}}{E_{\mathrm{tr1}}} = \frac{\mu_3 k_{\mathrm{tr}} - \mu_2 k_{\mathrm{out}}}{\mu_3 k_{\mathrm{tr}} + \mu_2 k_{\mathrm{out}}}\,\mathrm{e}^{2\mathrm{i}k_{\mathrm{tr}}h} =: \alpha_{\mathrm{T}},$$
$$\frac{E_{\mathrm{out}}}{E_{\mathrm{tr1}}} = \frac{2\mu_3 k_{\mathrm{tr}}}{\mu_3 k_{\mathrm{tr}} + \mu_2 k_{\mathrm{out}}}\,\mathrm{e}^{\mathrm{i}(k_{\mathrm{tr}}-k_{\mathrm{out}})h} =: \beta_{\mathrm{T}}. \tag{4.20}$$

On substituting $\alpha_{\mathrm{T}}$ into the first and second equations in Eq. (4.19), we find

$$\frac{E_{\mathrm{re}}}{E_{\mathrm{in}}} = \frac{\mu_2 k_{\mathrm{in}}(1+\alpha_{\mathrm{T}}) - \mu_1 k_{\mathrm{tr}}(1-\alpha_{\mathrm{T}})}{\mu_2 k_{\mathrm{in}}(1+\alpha_{\mathrm{T}}) + \mu_1 k_{\mathrm{tr}}(1-\alpha_{\mathrm{T}})},$$
$$\frac{E_{\mathrm{tr1}}}{E_{\mathrm{in}}} = \frac{2\mu_2 k_{\mathrm{in}}}{\mu_2 k_{\mathrm{in}}(1+\alpha_{\mathrm{T}}) + \mu_1 k_{\mathrm{tr}}(1-\alpha_{\mathrm{T}})} =: \gamma_{\mathrm{T}},$$
$$\frac{E_{\mathrm{out}}}{E_{\mathrm{in}}} = \beta_{\mathrm{T}}\gamma_{\mathrm{T}}. \tag{4.21}$$

Reflection and transmission coefficients are defined as in Eqs. (4.6) and (4.7), $R^{\mathrm{T,L}} = F^{\mathrm{T,L}}_{\mathrm{re}}/F^{\mathrm{T,L}}_{\mathrm{in}}$ and $T^{\mathrm{T,L}} := F^{\mathrm{T,L}}_{\mathrm{out}}/F^{\mathrm{T,L}}_{\mathrm{in}}$, so that the transversal ratios read

$$R^{\mathrm{T}} = |E_{\mathrm{re}}/E_{\mathrm{in}}|^2, \quad T^{\mathrm{T}} = \frac{\mu_1 k_{\mathrm{out}}}{\mu_3 k_{\mathrm{in}}}|\beta_{\mathrm{T}}\gamma_{\mathrm{T}}|^2. \tag{4.22}$$

As for the transmission coefficient, we assume real permeabilities and wave numbers in media 1 and 3, so that damping can only occur in the boundary layer, that is medium 2. If all three media are dielectrics, energy conservation applies, $R^{\mathrm{T}} + T^{\mathrm{T}} = 1$. In this case, the coefficients are periodic in $h$, the thickness of the boundary layer, and the extrema of $R^{\mathrm{T}}$ and $T^{\mathrm{T}}$ are determined by $\sin(2hk_{\mathrm{tr}}(\omega)) = 0$, the variation being with respect to the layer thickness, $\partial R^{\mathrm{T}}/\partial h = 0$. Thus the intensity minima and maxima occur at frequencies where the transversal wave number $k_{\mathrm{tr}} = \omega n_{\mathrm{T},2}$ is an integer multiple of $\pi/(2h)$; $n_{\mathrm{T},2}(\omega)$ is the transversal refractive index (2.13) of the layer. We find, for $\cos(2hk_{\mathrm{tr}}) = \pm 1$,

$$R^{\mathrm{T}}_{\cos=1} = \left(\frac{\mu_3 n_{\mathrm{T},1} - \mu_1 n_{\mathrm{T},3}}{\mu_3 n_{\mathrm{T},1} + \mu_1 n_{\mathrm{T},3}}\right)^2,$$
$$R^{\mathrm{T}}_{\cos=-1} = \left(\frac{\mu_2^2 n_{\mathrm{T},1} n_{\mathrm{T},3} - \mu_1\mu_3 n_{\mathrm{T},2}^2}{\mu_2^2 n_{\mathrm{T},1} n_{\mathrm{T},3} + \mu_1\mu_3 n_{\mathrm{T},2}^2}\right)^2, \tag{4.23}$$

where $\mu_i$ denotes the magnetic permeability and $n_{\mathrm{T},i}$ the transversal refractive index of the respective medium, cf. after Eq. (2.13). In the high-frequency limit $\omega \gg m_{\mathrm{t}}$, we substitute $n_{\mathrm{T}} \sim \sqrt{\varepsilon\mu}$ in Eq. (4.23),

$$R^{\mathrm{T}}_{\cos=1} \sim \left(\frac{\sqrt{\varepsilon_3\mu_1} - \sqrt{\varepsilon_1\mu_3}}{\sqrt{\varepsilon_3\mu_1} + \sqrt{\varepsilon_1\mu_3}}\right)^2,$$
$$R^{\mathrm{T}}_{\cos=-1} \sim \left(\frac{\mu_2\sqrt{\varepsilon_1\varepsilon_3} - \varepsilon_2\sqrt{\mu_1\mu_3}}{\mu_2\sqrt{\varepsilon_1\varepsilon_3} + \varepsilon_2\sqrt{\mu_1\mu_3}}\right)^2, \tag{4.24}$$

and in the low-frequency band $\omega \ll m_t$, we use $n_{\mathrm{T}} \sim \sqrt{\mu/\mu_0}\,m_t/\omega$ to obtain

$$R^{\mathrm{T}}_{\cos=1} \sim \left(\frac{\sqrt{\mu_{0,3}\mu_3} - \sqrt{\mu_{0,1}\mu_1}}{\sqrt{\mu_{0,3}\mu_3} + \sqrt{\mu_{0,1}\mu_1}}\right)^2,$$
$$R^{\mathrm{T}}_{\cos=-1} \sim \left(\frac{\mu_{0,2}\mu_2 - \sqrt{\mu_{0,1}\mu_1\mu_{0,3}\mu_3}}{\mu_{0,2}\mu_2 + \sqrt{\mu_{0,1}\mu_1\mu_{0,3}\mu_3}}\right)^2. \tag{4.25}$$

The meaning of these extremal transversal reflection coefficients and their longitudinal counterpart is discussed after Eq. (4.32).

#### 4.3.2. Longitudinal reflection and transmission coefficients

We proceed as in the previous case of transversal normal incidence, starting with the longitudinal boundary conditions, cf. Sections 3.2 and 4.2,

$$\varepsilon_1(E_{\mathrm{in}} + E_{\mathrm{re}}) = \varepsilon_2(E_{\mathrm{tr1}} + E_{\mathrm{tr2}}),$$
$$\frac{\varepsilon_1}{\varepsilon_{0,1}}k_{\mathrm{in}}(E_{\mathrm{in}} - E_{\mathrm{re}}) = \frac{\varepsilon_2}{\varepsilon_{0,2}}k_{\mathrm{tr}}(E_{\mathrm{tr1}} - E_{\mathrm{tr2}}),$$
$$\varepsilon_2(E_{\mathrm{tr1}}\mathrm{e}^{\mathrm{i}k_{\mathrm{tr}}h} + E_{\mathrm{tr2}}\mathrm{e}^{-\mathrm{i}k_{\mathrm{tr}}h}) = \varepsilon_3 E_{\mathrm{out}}\mathrm{e}^{\mathrm{i}k_{\mathrm{out}}h},$$
$$\frac{\varepsilon_2}{\varepsilon_{0,2}}k_{\mathrm{tr}}(E_{\mathrm{tr1}}\mathrm{e}^{\mathrm{i}k_{\mathrm{tr}}h} - E_{\mathrm{tr2}}\mathrm{e}^{-\mathrm{i}k_{\mathrm{tr}}h}) = \frac{\varepsilon_3}{\varepsilon_{0,3}}k_{\mathrm{out}}E_{\mathrm{out}}\mathrm{e}^{\mathrm{i}k_{\mathrm{out}}h}. \tag{4.26}$$

The third and fourth of these equations give

$$\frac{E_{\mathrm{tr2}}}{E_{\mathrm{tr1}}} = \frac{\varepsilon_{0,2}k_{\mathrm{out}} - \varepsilon_{0,3}k_{\mathrm{tr}}}{\varepsilon_{0,2}k_{\mathrm{out}} + \varepsilon_{0,3}k_{\mathrm{tr}}}\,\mathrm{e}^{2\mathrm{i}k_{\mathrm{tr}}h} =: \alpha_{\mathrm{L}},$$
$$\frac{E_{\mathrm{out}}}{E_{\mathrm{tr1}}} = \frac{\varepsilon_2}{\varepsilon_3}\frac{2\varepsilon_{0,3}k_{\mathrm{tr}}}{\varepsilon_{0,2}k_{\mathrm{out}} + \varepsilon_{0,3}k_{\mathrm{tr}}}\,\mathrm{e}^{\mathrm{i}(k_{\mathrm{tr}}-k_{\mathrm{out}})h} =: \beta_{\mathrm{L}}. \tag{4.27}$$

We substitute $\alpha_{\rm L}$ into the first and second equations in Eq. (4.26),

$$\frac{E_{\rm re}}{E_{\rm in}}=\frac{\varepsilon_{0,1}k_{\rm tr}(1-\alpha_{\rm L})-\varepsilon_{0,2}k_{\rm in}(1+\alpha_{\rm L})}{\varepsilon_{0,1}k_{\rm tr}(1-\alpha_{\rm L})+\varepsilon_{0,2}k_{\rm in}(1+\alpha_{\rm L})},$$

$$\frac{E_{\rm tr1}}{E_{\rm in}}=\frac{\varepsilon_1}{\varepsilon_2}\frac{2\varepsilon_{0,2}k_{\rm in}}{\varepsilon_{0,1}k_{\rm tr}(1-\alpha_{\rm L})+\varepsilon_{0,2}k_{\rm in}(1+\alpha_{\rm L})}=:\gamma_{\rm L},$$
$$\frac{E_{\rm out}}{E_{\rm in}}=\beta_{\rm L}\gamma_{\rm L}, \tag{4.28}$$

to find the longitudinal reflection and transmission coefficients, cf. Eq. (4.14),

$$R^{\rm L}=|E_{\rm re}/E_{\rm in}|^2,\quad T^{\rm L}=\frac{\varepsilon_3^2}{\varepsilon_1^2}\frac{\varepsilon_{0,1}}{\varepsilon_{0,3}}\frac{k_{\rm out}}{k_{\rm in}}|\beta_{\rm L}\gamma_{\rm L}|^2. \tag{4.29}$$

If all permeabilities are real, energy is conserved, $R^{\rm L}+T^{\rm L}=1$, and these coefficients are periodic in the layer thickness $h$. The intensity extrema of $R^{\rm L}$ and $T^{\rm L}$ are defined by the longitudinal wave number $k_{\rm tr}=\omega n_{\rm L,2}(\omega)$ in the layer, cf. Eqs. (2.10) and (2.13), occurring at frequencies solving $\cos(2hk_{\rm tr}(\omega))=\pm1$, analogously to Eq. (4.23):

$$R^{\rm L}_{\cos=1}=\left(\frac{\varepsilon_{0,2}^2n_{\rm L,1}n_{\rm L,3}-\varepsilon_{0,1}\varepsilon_{0,3}n_{\rm L,2}^2}{\varepsilon_{0,2}^2n_{\rm L,1}n_{\rm L,3}+\varepsilon_{0,1}\varepsilon_{0,3}n_{\rm L,2}^2}\right)^2,$$
$$R^{\rm L}_{\cos=-1}=\left(\frac{\varepsilon_{0,3}n_{\rm L,1}-\varepsilon_{0,1}n_{\rm L,3}}{\varepsilon_{0,3}n_{\rm L,1}+\varepsilon_{0,1}n_{\rm L,3}}\right)^2, \tag{4.30}$$

where $n_{{\rm L},i}$ is the longitudinal refractive index of the respective medium. At high frequencies, $\omega\gg m_{\rm t}$, we substitute $n_{\rm L}\sim\sqrt{\varepsilon_0\mu_0}$ to find the extremal reflection coefficients for longitudinal tachyons,

$$R^{\rm L}_{\cos=1}\sim\left(\frac{\varepsilon_{0,2}\sqrt{\mu_{0,1}\mu_{0,3}}-\mu_{0,2}\sqrt{\varepsilon_{0,1}\varepsilon_{0,3}}}{\varepsilon_{0,2}\sqrt{\mu_{0,1}\mu_{0,3}}+\mu_{0,2}\sqrt{\varepsilon_{0,1}\varepsilon_{0,3}}}\right)^2,$$
$$R^{\rm L}_{\cos=-1}\sim\left(\frac{\sqrt{\varepsilon_{0,3}\mu_{0,1}}-\sqrt{\varepsilon_{0,1}\mu_{0,3}}}{\sqrt{\varepsilon_{0,3}\mu_{0,1}}+\sqrt{\varepsilon_{0,1}\mu_{0,3}}}\right)^2. \tag{4.31}$$

In the low-frequency regime, we approximate $n_{\rm L}\sim\sqrt{\varepsilon_0/\varepsilon}m_t/\omega$ so that Eq. (4.30) simplifies to

$$R^{\rm L}_{\cos=1}\sim\left(\frac{\varepsilon_{0,2}\varepsilon_2-\sqrt{\varepsilon_{0,1}\varepsilon_1\varepsilon_{0,3}\varepsilon_3}}{\varepsilon_{0,2}\varepsilon_2+\sqrt{\varepsilon_{0,1}\varepsilon_1\varepsilon_{0,3}\varepsilon_3}}\right)^2,$$
$$R^{\rm L}_{\cos=-1}\sim\left(\frac{\sqrt{\varepsilon_{0,3}\varepsilon_3}-\sqrt{\varepsilon_{0,1}\varepsilon_1}}{\sqrt{\varepsilon_{0,3}\varepsilon_3}+\sqrt{\varepsilon_{0,1}\varepsilon_1}}\right)^2. \tag{4.32}$$

For example, we may set all permeabilities equal to one apart from the permittivity $\varepsilon_2$ of the layer. At high frequency, the longitudinal flux is almost totally transmitted since the leading order of the reflection coefficient vanishes, $R^{\rm L}_{\cos=\pm1}\approx0$. At low frequency, we still have $R^{\rm L}_{\cos=-1}\approx0$ (that is, for wave numbers $k_{\rm tr}=(l+1/2)\pi/h$ with integer $l$), but there is a non-vanishing fraction $R^{\rm L}_{\cos=1}\sim(\varepsilon_2-1)^2/(\varepsilon_2+1)^2$ of the incident flux reflected at frequencies satisfying $k_{\rm tr}(\omega)=l\pi/h$. This is just the opposite of the transversal case in Eqs. (4.24) and (4.25), where $R^{\rm T}_{\cos=-1}\sim(\varepsilon_2-1)^2/(\varepsilon_2+1)^2$ at high frequencies, whereas $R^{\rm T}_{\cos=\pm1}\approx0$ for $\omega\ll m_t$. More generally, there is a symmetry in the reflection coefficients (4.23) and (4.30) with regard to the interchange $\varepsilon_0\leftrightarrow\mu$, $\varepsilon\leftrightarrow\mu_0$, which is apparent in the asymptotic limits (4.24) and (4.31) as well as Eqs. (4.25) and (4.32). However, the extremal frequencies defined

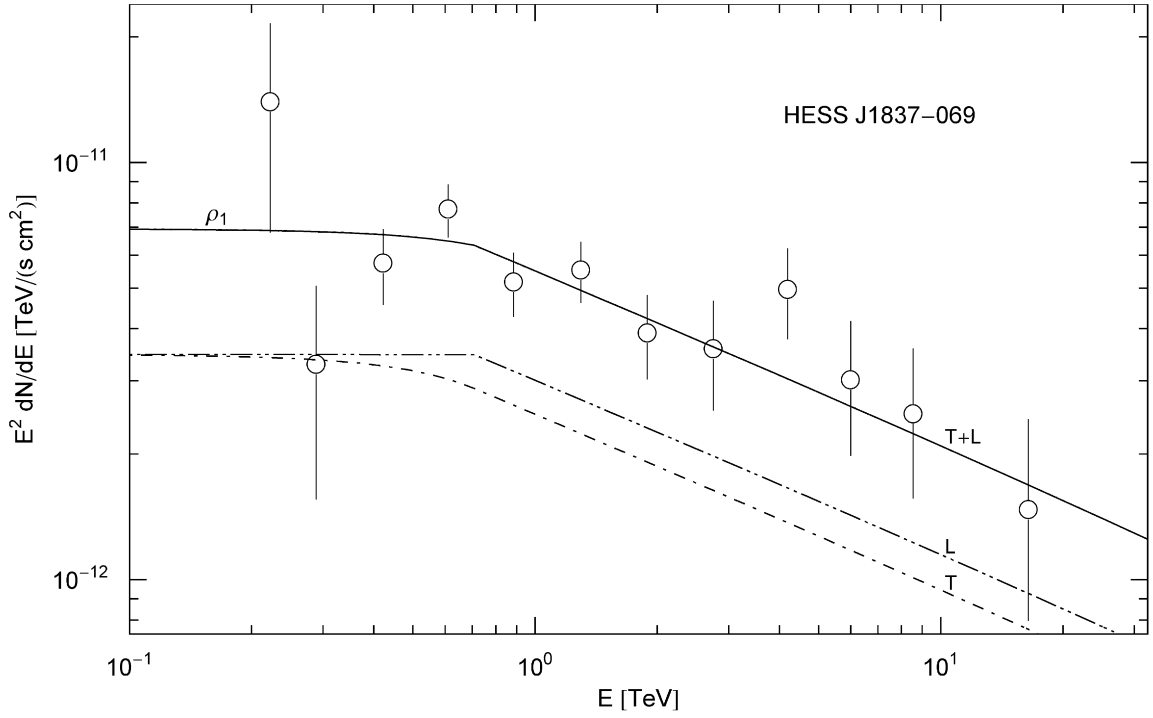


**Fig. 1.** Spectral map of the TeV $\gamma$-ray source HESS J1837−069 associated with the pulsar wind nebula AX J1838.0−0655. Flux points from Ref. [9]. The solid line depicts the unpolarized differential tachyon flux $dN^{\rm T+L}/dE$ rescaled with $E^2$ tachyon flux $dN^{\rm T+L}/dE$ rescaled with $E^2$, cf. (5.1). The transversal (dot-dashed) and longitudinal (double-dot-dashed) flux densities $dN^{\rm T,L}/dE$ add up to the total unpolarized flux cascade $\rho_1={\rm T}+{\rm L}$ generated by a nonthermal electron population. The cascade admits a power–law slope $\propto E^{1-\alpha}$ with electron index $\alpha\approx1.4$. A spectral break at $m_t\gamma_1\approx0.71$ TeV is visible as edge in the longitudinal component, where $m_t\approx2.15$ keV is the tachyon mass [6,18]. The least-squares fit is based on the unpolarized tachyon flux T+L, cf. Table 1.

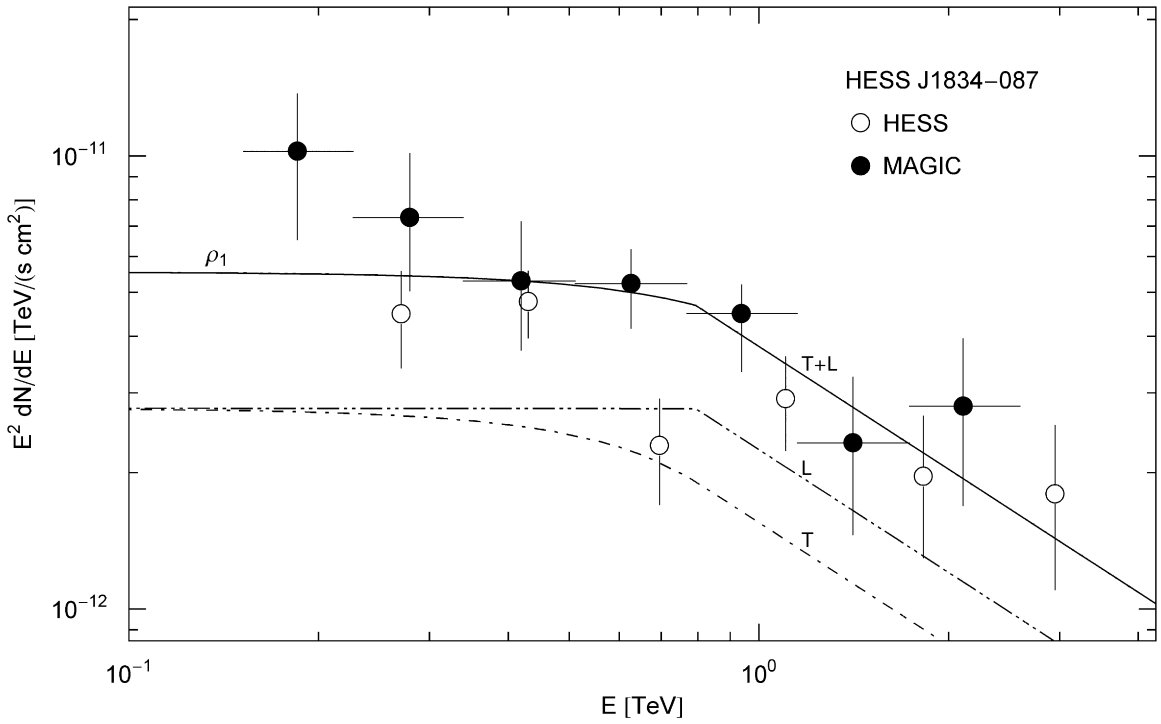


**Fig. 2.** Spectral map of the extended TeV source HESS J1834−087 in supernova remnant W41. HESS data points from Ref. [9], MAGIC points from Ref. [10]. Notation as in Fig. 1. The parameters of the shock-heated electron plasma are listed in Table 1. The spectral break in the longitudinal flux component (L) of the cascade occurs at 0.80 TeV. The distance estimate of this source is 4 kpc, and its electron index is 1.9, quite similar to the TeV source in Fig. 3 at a comparable distance. The power-law slope is steeper than of HESS J1837−069 at 6.6 kpc, cf. Fig. 1; there is no interstellar absorption of the tachyon flux [22].

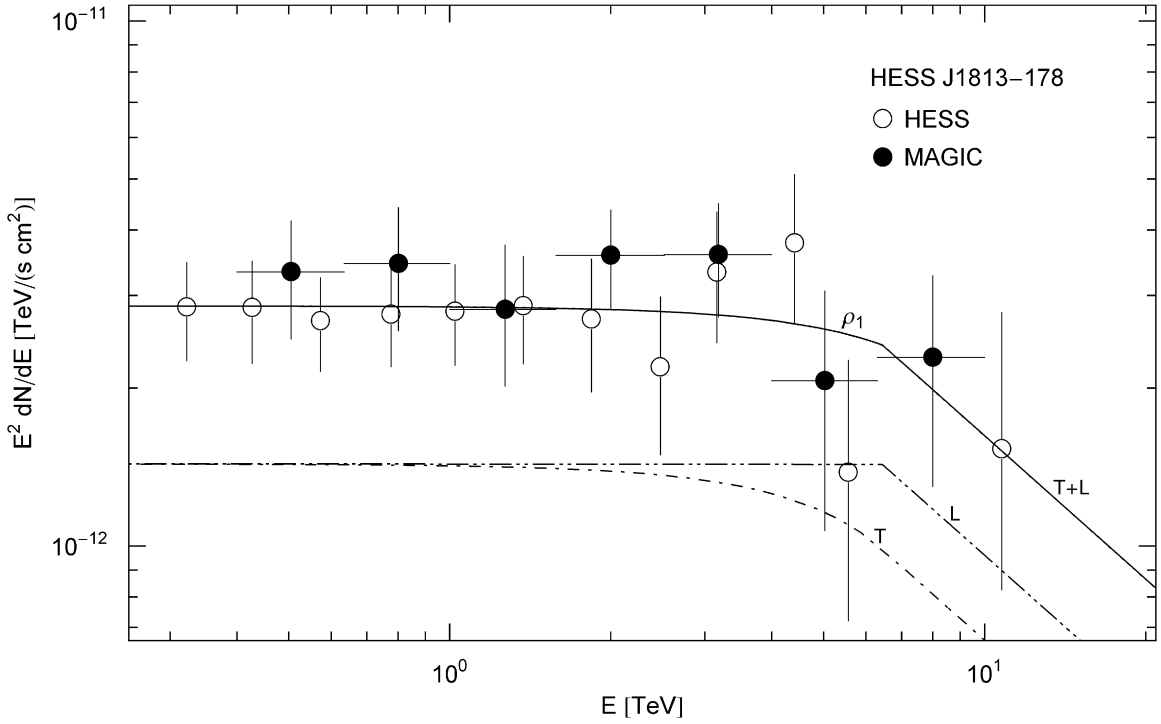


**Fig. 3.** Spectral map of the TeV $\gamma$-ray source HESS J1813−178 coincident with supernova remnant W33. HESS flux points from Ref. [9], MAGIC points from Ref. [11]. Notation as in Fig. 1. The tachyonic cascade $\rho_1 = \text{T+L}$ is generated by the ultra-relativistic electron plasma of the remnant, cf. Table 1. The spectral break at $m_t\gamma_1 \approx 6.5$ TeV separates the power-law slope from the extended GeV plateau distinctive of tachyonic cascade spectra [21,23,24].

**Table 1**
Parameters of the nonthermal electron plasma generating the tachyonic cascade spectra of the TeV γ-ray sources in Figs. 1–3.

| | $\alpha$ | $\gamma_1$ | $\hat{n}$ | $d$ (kpc) | $n^e$ |
|---|---|---|---|---|---|
| HESS J1837−069 | 1.4 | $3.3\times10^{8}$ | $7.5\times10^{-4}$ | 6.6 | $1.9\times10^{48}$ |
| HESS J1834−087 | 1.9 | $3.7\times10^{8}$ | $6.0\times10^{-4}$ | 4 | $5.5\times10^{47}$ |
| HESS J1813−178 | 1.9 | $3.0\times10^{9}$ | $3.1\times10^{-4}$ | 4.5 | $3.6\times10^{47}$ |

$\alpha$ is the electron index, and $\gamma_1$ the lower threshold Lorentz factor of the ultra-relativistic electron populations, cf. after Eq. (5.1). $\hat{n}$ determines the amplitude of the tachyon flux, from which the electron count $n^e$ is inferred at the indicated distance $d$, cf. Refs. [27–29]. The parameters $\alpha$, $\gamma_1$, and $\hat{n}$ are extracted from the $\chi^2$-fit T+L in the figures. The amplitude $\hat{n}$ is related to the electron number by $n^e \approx 5.75\times10^{49}\hat{n}d^2$ [kpc], cf. Ref. [7].

by the zeros of $\sin(2hk_{tr}(\omega))$ differ for transversal and longitudinal modes, unless the wave numbers (2.8) and (2.10) coincide in the layer.

## 5. Polarization components of tachyonic cascades radiated by a shock-heated electron plasma

Figs. 1–3 depict tachyonic cascade spectra of the TeV γ-ray sources HESS J1837−069, HESS J1834−087, and HESS J1813−178. The cascades are plots of the $E^2$-rescaled flux densities,

$$E^2\frac{dN^{T,L}}{dE}=\frac{\omega}{4\pi d^2}\langle p^{T,L}(\omega)\rangle, \tag{5.1}$$

where $d$ is the distance to the source, and $\langle p^{T,L}(\omega=E/\hbar)\rangle$ the transversal/longitudinal tachyonic spectral density averaged over a nonthermal electronic power-law distribution, $d\rho_{\alpha,\beta}\propto\gamma^{-\alpha-1}e^{-\beta\gamma}\sqrt{\gamma^2-1}\,d\gamma$ [21]. As for the latter, $\alpha$ is the electronic power-law index, the ultra-relativistic electronic Lorentz factors range in an interval $\gamma_1\leqslant\gamma<\infty$, $\gamma_1\gg1$, and the exponential cutoff is related to the electron temperature by $\beta=mc^2/(kT)$. A thermal Maxwell–Boltzmann distribution corresponds to $\alpha=-2$ and $\gamma_1=1$. The least-squares fit is performed with the unpolarized flux density $dN^{T+L}=dN^T+dN^L$, and then split into transversal and longitudinal radiation components. The details of the spectral fitting have been explained in Ref. [22]. The parameters of the electron distributions $d\rho_{\alpha,\beta}$ generating the tachyonic cascades are listed in Table 1. The cutoff parameter $\beta$ in the Boltzmann factor could not be extracted from the presently available flux points, in contrast to the power–law index $\alpha$ and the lower edge $\gamma_1$ of Lorentz factors. The power–law slope ultimately terminates in exponential decay, cf. the spectral map of HESS J1825−137 in Fig. 5 of Ref. [7]. As for the spectral fits in Figs. 1–3, there is no downward bend yet in the presently accessible TeV range.

Fig. 1 shows the TeV spectral map of the unidentified TeV source HESS J1837−069 [9], coincident with the pulsar wind nebula AX J1838.0−0655. The distance estimate to this X-ray nebula is 6.6 kpc, by association with a nearby cluster of red supergiants. Fig. 2 depicts the spectral fit to the extended TeV source HESS J1834−087, associated with the shell-type supernova remnant W41, cf. Refs. [9,10]. The kinematic distance estimate of W41 is 4 kpc. Spectral plateaus in the MeV to GeV range occur frequently in spectral maps of both thermal and nonthermal TeV sources, and can easily be fitted with tachyonic cascade spectra, in contrast to electromagnetic or hadronic radiation models. Thermal spectra of γ-ray binaries such as binary pulsars and microquasars are studied in Refs. [12,23], and a thermal cascade fit of a γ-ray quasar is performed in Ref. [24]. The shocked electron plasma of supernova remnants requires nonthermal electron densities. Fig. 3 shows a nonthermal cascade fit to the TeV source HESS J1813−178, located in the vicinity of the H II region W33 [9,11] at a distance of 4.5 kpc. The lower edge of Lorentz factors of the electron plasma is $\gamma_1\approx3.0\times10^9$, inferred from the cascade fit. The corresponding electron and proton energies are $m_e\gamma_1\approx1.5\times10^{15}$ eV and $m_p\gamma_1\approx2.8\times10^{18}$ eV. These lower bounds on the energy of the radiating source particles are to be compared to the spectral breaks in the cosmic-ray spectrum at $10^{15.5}$ and $10^{17.8}$ eV, dubbed knee and second knee, respectively [25,26]. The bounds are one order lower for the sources in Figs. 1 and 2, cf. Table 1, but in all three remnants the lower bound on the proton energy is close to the second knee.

## 6. Conclusion

We have studied the refraction of superluminal radiation at dielectric interfaces, in particular the refraction angles for transversal and longitudinal incidence, and the dependence of the transmission and reflection coefficients on the polarization of the incident radiation modes. Speed and energy of tachyonic quanta are related by $\omega=m_t(v_{gr}^2-1)^{-1/2}$ in vacuum, cf. after Eq. (2.12). At γ-ray energies, their speed is close to the speed of light, the basic difference to electromagnetic radiation being the longitudinally polarized flux component. The polarization of tachyons can be determined from the refraction angles at dielectric interfaces, cf. after Eq. (4.1), or from the reflection coefficients, which greatly differ for transversal and longitudinal modes, cf. after Eq. (4.32). We performed tachyonic cascade fits to the γ-ray spectra of the TeV sources in Figs. 1–3, and disentangled the transversal and longitudinal flux components.

Shocked electron plasmas generate nonthermal γ-ray cascades typical for supernova remnants and pulsar wind nebulae. The characteristic feature is the extended spectral plateau at GeV energies, followed by a steep but barely bent spectral slope in the low TeV range, assuming a double-logarithmic and $E^2$-rescaled flux representation as in Figs. 1–3. The spectral maps discussed here are to be compared to the unpulsed γ-ray spectrum of the Crab Nebula, cf. Fig. 1 in Ref. [18], the spectral map of supernova remnant RX J1713.7−3946 in Fig. 2 of Ref. [18], the spectra of HESS J1825−137 and TeV J2032+4130 in Figs. 5 and 6 of Ref. [7], and the extended γ-ray cascade of supernova remnant W28 in Fig. 4 of Ref. [22]. All these spectra show GeV plateaus followed by straight or slightly curved power–law slopes. Traditional radiation mechanisms such as inverse Compton scattering or proton–proton scattering followed by pion decay fail to reproduce the extended plateaus in the spectral maps, a fact often concealed by compression in broadband maps. By contrast, tachyonic cascades provide excellent fits to the GeV plateaus and power–law slopes. The latter are a signature of shock-heated electron plasmas, and absent in the spectra of thermal γ-ray sources like TeV blazars [30,31], where the plateaus terminate in exponential decay without power–law transition. The spectral breaks at the join of the spectral plateaus and the power–law slopes are determined by the lower threshold Lorentz factors of the nonthermal source populations in the remnants. These Lorentz factors can be extracted from the spectral fits [32], and suggest that TeV γ-ray sources in Galactic supernova remnants are capable of accelerating protons to energies above the spectral break at $10^{17.8}$ eV in the cosmic-ray spectrum.

## Acknowledgments

The author acknowledges the support of the Japan Society for the Promotion of Science. The hospitality and stimulating atmosphere of the Centre for Nonlinear Dynamics, Bharathidasan University, Trichy, and the Institute of Mathematical Sciences,

Chennai, are likewise gratefully acknowledged. I also thank the referee for useful suggestions regarding substance as well as readability, which greatly helped to improve the initial draft.

## References

[1] J.A. Wheeler, R.P. Feynman, Rev. Mod. Phys. 17 (1945) 157.
[2] S. Tanaka, Prog. Theor. Phys. 24 (1960) 171.
[3] Ya.P. Terletsky, Sov. Phys. Dokl. 5 (1961) 782.
[4] R. Newton, Science 167 (1970) 1569.
[5] K. Kamoi, S. Kamefuchi, Prog. Theor. Phys. 45 (1971) 1646.
[6] R. Tomaschitz, European Phys. J. B 17 (2000) 523.
[7] R. Tomaschitz, Ann. Phys. 322 (2007) 677.
[8] R. Tomaschitz, European Phys. J. D 32 (2005) 241.
[9] F. Aharonian, et al., Astrophys. J. 636 (2006) 777.
[10] J. Albert, et al., Astrophys. J. 643 (2006) L53.
[11] J. Albert, et al., Astrophys. J. 637 (2006) L41.
[12] R. Tomaschitz, Phys. Lett. A 366 (2007) 289.
[13] L.D. Landau, E.M. Lifshitz, Electrodynamics of Continuous Media, Pergamon Press, Oxford, 1984.
[14] M. Born, E. Wolf, Principles of Optics, Cambridge University Press, Cambridge, 2003.
[15] A. Lagarkov, V. Kisel, Phys. B 394 (2007) 163.
[16] G. Xu, et al., Phys. B 403 (2008) 3417.
[17] L.-Y. Wu, L.-W. Chen, R.C.-C. Wang, Phys. B 403 (2008) 3599.
[18] R. Tomaschitz, European Phys. J. C 49 (2007) 815.
[19] J.A. Adam, Phys. Rep. 356 (2002) 229.
[20] J.A. Stratton, Electromagnetic Theory, Wiley–IEEE Press, New York, 2007.
[21] R. Tomaschitz, Phys. A 387 (2008) 3480.
[22] R. Tomaschitz, Phys. Lett. A 372 (2008) 4344.
[23] R. Tomaschitz, Phys. A 385 (2007) 558.
[24] R. Tomaschitz, EPL 84 (2008) 19001.
[25] J.W. Cronin, Nucl. Phys. B (Proc. Suppl.) 138 (2005) 465.
[26] M. Nagano, A.A. Watson, Rev. Mod. Phys. 72 (2000) 689.
[27] B. Davies, et al., Astrophys. J. 676 (2008) 1016.
[28] W.W. Tian, et al., Astrophys. J. 657 (2007) L25.
[29] D.J. Helfand, et al., Astrophys. J. 665 (2007) 1297.
[30] R. Tomaschitz, EPL 85 (2009) 29001.
[31] R. Tomaschitz, Opt. Commun. (2009), doi:10.1016/j.optcom.2009.01.024.
[32] R. Tomaschitz, Astropart. Phys. 27 (2007) 92.